

Geochemistry, Geophysics, Geosystems®




RESEARCH ARTICLE

10.1029/2025GC012319

Origin of Silicic Magmatism at the Katla Volcanic Complex, South Iceland

Key Points:

- The study provides new $\delta^{18}\text{O}$ values for nearly 60 volcanic rocks from Katla, ranging from basaltic to silica-rich samples
- Basaltic samples show MORB-like $\delta^{18}\text{O}$, while silicic rocks have low (sub-MORB) $\delta^{18}\text{O}$ due to interaction with low- $\delta^{18}\text{O}$ Icelandic crust
- Two-stage magma evolution with fractionation of basaltic magma in mid-crust followed by assimilation of altered crust at shallow levels

Valentin R. Troll^{1,2} , Frances M. Deegan^{1,2} , Jussi S. Heinonen^{3,4} , Caroline Svanholm¹, Chris Harris⁵, Christian M. Lacasse⁶, Harri Geiger⁷ , Agata Poganj¹ , Louise Thomas⁸, Malin Andersson¹, Romain Meyer⁹ , and Thorvaldur Thordarson¹⁰ 

¹Department of Earth Sciences, Uppsala University, Natural Resources & Sustainable Development, Uppsala, Sweden, ²Centre for Natural Hazards and Disaster Science (CNDS), Uppsala University, Uppsala, Sweden, ³Åbo Akademi University, Geology and Mineralogy, Åbo, Finland, ⁴Department of Geoscience and Geography, University of Helsinki, Helsinki, Finland, ⁵Department of Geological Sciences, University of Cape Town, Rondebosch, South Africa, ⁶SQN 412, Brasília, Brazil, ⁷Institute of Earth and Environmental Sciences, University of Freiburg, Freiburg im Breisgau, Germany, ⁸Faculty of Science, Technology, Engineering & Mathematics, The Open University, Milton Keynes, England, ⁹Service géologique du Luxembourg, Bertrange, Luxembourg, ¹⁰Faculty of Earth Sciences, University of Iceland, Reykjavík, Iceland

Supporting Information:

Supporting Information may be found in the online version of this article.

Correspondence to:

V. R. Troll,
valentin.troll@geo.uu.se

Citation:

Troll, V. R., Deegan, F. M., Heinonen, J. S., Svanholm, C., Harris, C., Lacasse, C. M., et al. (2025). Origin of silicic magmatism at the Katla volcanic complex, South Iceland. *Geochemistry, Geophysics, Geosystems*, 26, e2025GC012319. <https://doi.org/10.1029/2025GC012319>

Received 26 MAR 2025

Accepted 5 MAY 2025

Author Contributions:

Conceptualization: Valentin R. Troll
Data curation: Valentin R. Troll, Frances M. Deegan, Jussi S. Heinonen, Caroline Svanholm
Formal analysis: Valentin R. Troll, Frances M. Deegan, Jussi S. Heinonen, Caroline Svanholm, Chris Harris
Funding acquisition: Valentin R. Troll, Frances M. Deegan
Investigation: Valentin R. Troll, Frances M. Deegan, Jussi S. Heinonen, Caroline Svanholm, Chris Harris, Harri Geiger

Abstract The Katla volcano is a bimodal caldera complex within Iceland's basalt-dominated Eastern Volcanic Zone. To unravel the petrogenesis of silica-rich rocks from Katla, we provide new $\delta^{18}\text{O}$ values for almost 60 basaltic, intermediate, and high-silica eruptive rocks, including a number of partially melted felsic xenoliths. The basaltic samples display a range in bulk-rock $\delta^{18}\text{O}$ values from +4.3 to +8.5‰ ($n = 17$) and the sparse intermediate samples from +4.1 to +5.9‰ ($n = 3$). In turn, silicic rock samples and feldspar separates range from +2.7 to +6.4‰ ($n = 38$), whereas felsic xenoliths yield the lowest values from -4.9 to -2.3‰ ($n = 4$). The majority (95%) of the Katla silicic volcanics have $\delta^{18}\text{O}$ values below typical MORB (i.e., ≤ 5.0 ‰), ruling out an origin via closed-system fractional crystallization from the basaltic magmas. We utilized the new $\delta^{18}\text{O}$ values to model possible assimilation and fractional crystallization (AFC) scenarios. The results indicate an early stage of FC/AFC at deep- to mid-crustal levels, followed by assimilation of low- $\delta^{18}\text{O}$ hydrothermally altered sub-volcanic materials similar to the low- $\delta^{18}\text{O}$ felsic xenoliths at shallow crustal levels. Such a two-stage magma evolution is consistent with available geophysical and geobarometry studies at Katla, indicating mid- to deep-crustal and shallow-crustal magma domains. Importantly, mafic rocks dominantly show MORB-like $\delta^{18}\text{O}$ values, whereas low $\delta^{18}\text{O}$ values occur essentially in silicic rocks only. This implies that the low- $\delta^{18}\text{O}$ values at Katla are imposed by interaction with the Icelandic crust rather than reflecting low $\delta^{18}\text{O}$ mantle sources.

Plain Language Summary Iceland is a basalt-dominated volcanic province, but central volcanoes such as Katla show abundant silicic rock compositions. To better understand how Katla's silica-rich rocks form, we measured oxygen isotope values ($\delta^{18}\text{O}$) of about 60 rock samples, including basalt, intermediate, and silica-rich rocks, as well as plutonic rock fragments found in the lavas. The basalts show mantle-like $\delta^{18}\text{O}$ values, while intermediate rocks display a similar but smaller range. The silica-rich rocks show the broadest range of values, whereas the plutonic rock fragments have the lowest values of all the samples analyzed. Moreover, most of the silica-rich rocks from Katla have oxygen isotope values below those of typical basaltic rocks, which suggests that they did not form by closed system evolution alone. The most likely explanation is that evolving magmas rose from depth via several storage levels and eventually interacted with low $\delta^{18}\text{O}$ altered materials from the shallower parts of the volcanic edifice. This two-step process agrees with studies on Katla's interior through seismic tomography, which shows different areas of magma residence at both deeper and shallower levels. We conclude that the low oxygen isotope values in Katla's silica-rich rocks seem to result from interactions with local crust and not from deep mantle sources.

© 2025 The Author(s). Geochemistry, Geophysics, Geosystems published by Wiley Periodicals LLC on behalf of American Geophysical Union.

This is an open access article under the terms of the [Creative Commons Attribution License](https://creativecommons.org/licenses/by/4.0/), which permits use, distribution and reproduction in any medium, provided the original work is properly cited.

1. Introduction

Basaltic lithologies dominate the Icelandic surface geology (>80%). Silicic rocks are present in smaller amounts (c. 15%), and only <5% intermediate igneous rocks are mapped, thus defining a pronounced compositional gap (Carmichael, 1964; Jakobsson, 1979; Walker, 1966). Iceland is located in a basaltic oceanic rift setting situated on top of the Mid-Atlantic Ridge, and so the amount of silicic eruptive material is unusually large for an oceanic island. Consequently, Iceland is widely considered a type-locality of bimodal magmatism (e.g., I. Bindeman

Methodology: Valentin R. Troll, Frances M. Deegan, Jussi S. Heinonen, Chris Harris

Resources: Valentin R. Troll, Christian M. Lacasse, Louise Thomas

Supervision: Valentin R. Troll

Validation: Valentin R. Troll, Frances M. Deegan, Jussi S. Heinonen, Chris Harris, Harri Geiger

Visualization: Valentin R. Troll, Jussi S. Heinonen, Caroline Svanholm, Thorvaldur Thordarson

Writing – original draft: Valentin R. Troll

Writing – review & editing: Valentin R. Troll, Frances M. Deegan, Jussi S. Heinonen, Caroline Svanholm, Chris Harris, Christian M. Lacasse, Harri Geiger, Agata Poganj, Louise Thomas, Malin Andersson, Romain Meyer, Thorvaldur Thordarson

et al., 2012; Bunsen, 1851; Charreteur et al., 2013; Sigurdsson, 1977). Katla volcano in South Iceland is one of the most prolific volcanic complexes in the active volcanic rift zone in Iceland and displays a varied eruptive history, involving frequent basaltic tephra eruptions but also silica-rich eruptive events (e.g., Budd et al., 2016; Lacasse et al., 1995, 2007; Larsen et al., 2001; Thordarson & Höskuldsson, 2008; Óladóttir et al., 2008). Under current climatic conditions with prevailing north-westerly winds, a future major felsic explosive eruption at Katla could be a notable volcanic event in the North Atlantic region (e.g., Harning et al., 2024 and references therein), with potentially severe local and regional effects, including disruption of air traffic across large swathes of Northern Europe.

The origin of silica-rich explosive rocks at Katla is not yet fully resolved, and two main petrogenetic models are currently discussed. The first model involves extraction of an evolving assemblage of mineral phases by fractional crystallization (FC) from a basaltic parent mantle melt, whereby the residual magma gets progressively more evolved while the extracted mineral phases (e.g., olivine, clinopyroxene, plagioclase, apatite, ilmenite, titanomagnetite, K-feldspar) are concentrated in deeper crustal cumulate lithologies (e.g., Carmichael, 1964; Furman et al., 1992; Jónasson, 2005; MacDonald et al., 1990). Fractional crystallization during multiple stages coupled with magma mixing and hybridization has also been proposed (e.g., Blake, 1984; Macdonald et al., 1990; Sigurdsson & Sparks, 1981), which represents a variation of the classic FC scenario. The second model is based on partial melting of rocks at crustal levels involving either plagiogranite or hydrothermally altered basaltic rocks (e.g., I. Bindeman et al., 2012; Gunnarsson et al., 1998; Lacasse et al., 2007; Muehlenbachs et al., 1974; Óskarsson et al., 1982; Pope et al., 2013; Rasmussen et al., 2022; Sigmarsson et al., 1991; Sigurdsson, 1977). Quenched xenoliths in Iceland that record different stages of remelting as the result of heterogeneous melting of crustal compositions are the main line of support for this model, and include trondhjemite, gabbro, and leucocratic granodiorite lithologies (Geiger et al., 2016; Gunnarsson et al., 1998; Gurenko et al., 2015).

Another line of investigation explores the unusually widespread occurrence of sub-mantle “low- $\delta^{18}\text{O}$ magmas” throughout Iceland. Specifically, compared to mid-ocean ridge (MORB; c. 5.5‰) basalts, the $\delta^{18}\text{O}$ values of central Iceland basaltic rocks are often remarkably low (I. N. Bindeman et al., 2022; Muehlenbachs & Clayton, 1972; Pope et al., 2013; Rasmussen et al., 2022; Winpenny & MacLennan, 2014). This can be explained by either relatively low primary mantle $\delta^{18}\text{O}$ values under Central Iceland, perhaps down to ca. +4‰, or by the northerly cold oceanic climate in Iceland, which generates high rates of precipitation. The latter, in combination with crustal extension, active volcanism, and crustal remelting, promotes deep meteoric-hydrothermal systems and produces an extensively altered crust to a depth of ≥ 3 km with $\delta^{18}\text{O}$ values down to lower than 0‰ (e.g., I. Bindeman et al., 2012; Eiler, 2001; Hattori & Muehlenbachs, 1982; Muehlenbachs et al., 1974). The magnitude of ^{18}O -depletion of the various crustal rocks in this setting depends on specific water/rock ratios in different hydrothermal systems and stronger depletion results from higher rates of interaction with circulating low- $\delta^{18}\text{O}$ meteoric and geothermal waters. Notably, the resulting low- $\delta^{18}\text{O}$ altered rocks are common at central volcanoes (Hattori & Muehlenbachs, 1982). In contrast, $\delta^{18}\text{O}$ values above +7‰ are rarely found in igneous rocks in Iceland (e.g., Berg et al., 2018; I. Bindeman et al., 2008), and $\delta^{18}\text{O}$ values of igneous rocks which exceed the range generated by closed-system fractionation of mantle-derived magmas (+5.7 to c. +7‰; Valley et al., 2005; I. Bindeman et al., 2008) have usually either experienced low-temperature isotope exchange or assimilated low-temperature altered material (or a combination of these).

The main focus of petrological investigations at Katla volcano has been on the mafic end of the eruptive spectrum (e.g., I. Bindeman et al., 2008; Óladóttir et al., 2008, 2018; Thordarson et al., 2001). The silicic compositions are an important part of the Katla volcanic system; however, considering that six silicic eruptions from Katla have been correlated with the largest layers of the extensive North Atlantic Ash Zone One (Larsen et al., 2001). The controversial origin of high-silica rocks in Iceland led us to investigate a large suite of mafic to silica-rich rocks, plus several mineral and tephra samples from Katla volcano for their oxygen isotope ratios. We present a total of 62 new $\delta^{18}\text{O}$ values to complement existing major and trace element as well as radiogenic isotope data on the same sample suite (see Budd, 2015; Lacasse et al., 2007). The new isotope data help to test existing geochemical and geophysical models of the inner workings of Katla volcano and refine our understanding of the petrogenesis of silica-rich Katla rocks and thus contribute to the wider debate on silicic rock formation in Iceland. In addition, the new oxygen isotope data enable us to assess open versus closed system differentiation processes as well as the origin of mafic Katla magmas, and the new data will thus help to better understand the intrinsic volcanic behavior of the Katla system through time.

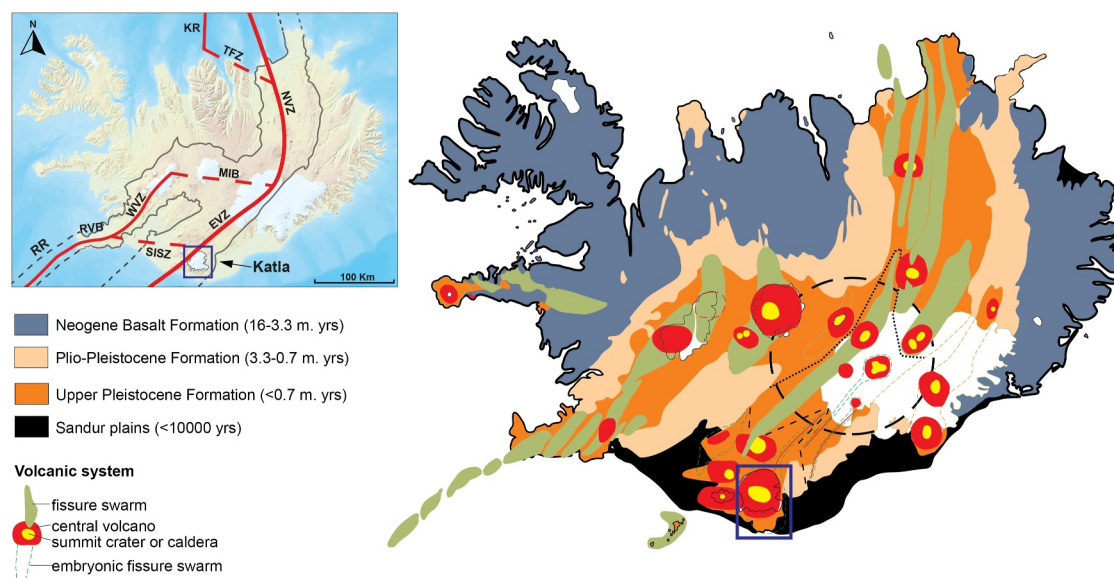


Figure 1. Geological overview map of Iceland showing Ages of basalt formations and locations of volcanic systems. Katla is one of the larger volcanic systems in Iceland and is located near the southern tip of the island (blue box). The inset (top right) shows the active volcanic zones and structural elements after A. Gudmundsson (2007), comprising the Northern Volcanic Zone (NVZ), Eastern Volcanic Zone (EVZ), Western Volcanic Zone (WVZ), Mid-Iceland Belt (MIB), Reykjanes Volcanic Belt (RVB), Reykjanes Ridge (RR), South Iceland seismic zone (SISZ), Tjörnes Fracture Zone (TFZ), and Kolbeinsey Ridge (KR). The location of Katla is marked by a green box.

2. Geological Background

2.1. Geological Setting of Katla Volcano

Katla central volcano in South Iceland is located to the east of the Eyjafjallajökull volcano within the Eastern Volcanic Zone (EVZ) of Iceland (Figure 1) and is situated largely beneath the Mýrdalsjökull ice cap (Björnsson et al., 2000; Larsen et al., 2001). The sub-ice topography of the area was mapped by radio echo soundings by Björnsson et al. (2000), which revealed a 14 km diameter subglacial caldera enclosing an area of c. 100 km² with a depth of 600–750 m. The caldera rim reaches 1,380 m.a.s.l. and is shaped by three major glaciers. Numerous major subglacial ridges as well as several 750 to 1,100 m high individual peaks can be distinguished geomorphologically from the caldera rim. The topographic highs are thought to have resulted from subglacial eruptions on the caldera floor or along the caldera rim (Björnsson et al., 2000). Katla is considered one of the most productive volcanoes in Iceland and has erupted over 180 times during the Holocene with individual eruption volumes of tephra of up to 1.5 km³ (Thordarson & Höskuldsson, 2008). Eruption frequencies between 10 and 30 times per millennium were reported for the period of the past 8.4 ky (Óladóttir et al., 2008). These were dominantly basaltic, but at least 17 of the Holocene eruptions at Katla comprised dacitic and rhyolitic magma (Larsen et al., 2001). A series of at least five rhyolitic Plinian eruptions took place in the time interval between 12.3 and 11.2 ka (e.g., Harning et al., 2024), including the 12.3 ka Vedde Ash eruption (Blockley et al., 2007) and the slightly younger Sólheimar ignimbrite event. The former dispersed tephra over large swaths of the European continent, reaching as far as the Balkan Peninsula, while the testament of the latter is c. 7 km³ of pyroclastic deposits that blanket the southern slopes of the volcano (Blockley et al., 2007; Lacasse et al., 1995; Tomlinson et al., 2012). The felsic magma that erupted since, referred to as SILK (= silicic Katla events), are dacitic in composition and show more restricted tephra volumes of 0.01–0.3 km³ (Larsen et al., 2001; Óladóttir et al., 2008). The most recent subaerial pyroclastic eruption occurred in 1918 (Budd et al., 2016; Sturkell et al., 2008, 2010) and lasted 24 days, generating a ~14 km high eruption column (M. T. Gudmundsson et al., 2021; Larsen, 2000).

2.2. Summary of Previous Work

A simple plumbing system at Katla was suggested by previous petrological studies that considered the volcano to be directly fed with magma from lower- to mid-crustal levels and at present a magma storage/chamber at shallow crustal depths was considered unlikely (Óladóttir et al., 2005, 2008). A seismic anomaly and a non-magnetic body

were recognized at c. 5 km below the summit of Katla, however, indicating a shallow magma pocket or reservoir to underlie the volcano. Moreover, an intruding silicic cryptodome has been recognized at shallow crustal levels beneath the volcano based on seismic anomalies (O. Gudmundsson et al., 1994; Jeddi et al., 2016, 2017; Jónsson & Kristjánsson, 2000; Soosalu et al., 2006). Provided a silicic magma reservoir exists beneath the Katla caldera, a scenario similar to that of the Eyjafjallajökull volcano is plausible, where during the 2010 eruption remobilization of an older and more evolved magma reservoir was caused by injection of mafic magma (cf. Sigmarsson et al., 2011; Sigmundsson et al., 2010). Most recent mineral-melt thermobarometry studies of eruptive basaltic materials from Katla indicate a shallow-level (≤ 8 km depth) as well as a deep- to mid-crustal (≤ 20 km depth) magma reservoir beneath the caldera, hinting at a two-tiered plumbing system (Budd et al., 2016; Kelley & Barton, 2008). Pilot studies of combined geobarometry modeling and oxygen isotope data of eruptive material from Katla suggested a ~ 10 km crystallization depth for basaltic magma with mantle-like $\delta^{18}\text{O}$ -values, that is, $\sim +5.8\text{‰}$, that is feeding a shallower silicic reservoir at ~ 3 km with relatively low $\delta^{18}\text{O}$ -values of $\sim +3.8\text{‰}$ (Budd, 2015).

3. Sample Set

A suite of 62 basaltic to silica-rich rocks as well as tephra and mineral samples derived from Katla were used in this study (Figures S1 and S2 in Supporting Information S1). The samples were previously characterized by Lacasse et al. (2007) and Budd (2015). The presented data comprise 52 new oxygen isotope analyses from the samples of Lacasse et al. (2007), which were combined with pilot oxygen data presented in Budd (2015) ($n = 10$) (Table 1; Figure 2). In detail, the oxygen isotope analyses presented here comprise basaltic ($n = 17$), intermediate ($n = 3$), and silicic bulk rocks ($n = 33$) in addition to feldspar separates extracted from silicic rocks ($n = 5$) and several felsic plutonic xenoliths ($n = 4$). Sampled areas cover the Mýrdalsjökull glacial ice cap and the ice-free land southward toward the coast, involving lava sequences, pyroclastic rocks and jökulhlaup deposits (Figure 2). The exposures include (a) basaltic lava flows, (b) ice-free rhyolitic lava sequences at Bláfell, Gvendarfell, Kriki, and a nunatak at Austmannsbunga, (c) exposures of pyroclastic rocks from the last silicic eruption at ~ 12 ky at Enta, Huldufjöll, Dalárgil, Húsargil and Rjúpnagil, (d) layers of historical and prehistoric tephra falls (e.g., the 1918 eruption), and (e) jökulhlaup deposits at Skógsandur and Dyrhólaey (Budd, 2015; Budd et al., 2016; Lacasse et al., 2007). Five silicic rock samples were selected for feldspar separation. The feldspar separates were hand-picked from whole rocks, and subsequently also analyzed for oxygen isotopes, allowing mineral-rock equilibrium to be assessed (Table 1). There are no systematic age constraints available on the rock samples, but the nunataks that are in the vicinity of and protrude Mýrdalsjökull Glacier are known to be pre-Holocene in age (i.e., samples KAT01-A, KAT01-B, KAT02-18, KAT02-19a, KAT02-19b, KAT02-20, IC95-132, IC95-193, IC95-194; Lacasse et al., 2007; Figure 2), whereas the tephra samples from Budd et al. (2016) were dated at 8, 4.22, and 1.25 ky and include a sample from the historical 1918 eruption.

Whole-rock major and trace element data as well as radiogenic isotope data from Budd (2015), Budd et al. (2016), and Lacasse et al. (2007) were employed for this study. The compiled whole-rock data set can be found in Data Set S1. The SiO_2 range of the Katla basaltic suite of our study varies between 43 and 51 wt.% and the rocks display slightly alkaline characteristics and fall within the basalt and microbasalt fields on a total alkali versus silica (TAS) plot (Figure 3). The silicic volcanics and xenoliths of the Katla lavas range between 67 and 72 wt.% SiO_2 and plot as dominantly subalkaline rhyolites and subalkaline trachydacites (Figure 3). Compositions of the silicic volcanics show limited variability in Al_2O_3 (12.8–13.9 wt.%), TiO_2 (< 0.5 wt.%), Fe_2O_3 (2.0–5.3 wt.%), MnO (< 0.2 wt.%), MgO (< 0.4 wt.%), CaO (0.5–2 wt.%) and $\text{Na}_2\text{O} + \text{K}_2\text{O}$ (8.2–9.9 wt.%) (Data Set S1). Samples of intermediate composition are rare and classify as basaltic andesite and trachyte/trachydacite, with SiO_2 compositions between 56 and 66 wt.%.

Whole-rock trace element concentrations of the Katla samples are shown in a multielement variation diagram normalized to primitive mantle (Figure 4) and the full trace element and rare earth element data are given in Data Set S1. The basaltic samples display a comparatively narrow compositional range with a strong enrichment relative to E-MORB (see also Lacasse et al., 2007). Published data for basaltic tephra differ from the basaltic sample suite we present, and may link to Holocene tephra at Katla being generally aphyric, contrasting pre-Holocene lavas and tephra. The silicic suite displays a distinct enrichment in light rare earth elements (LREE) compared to heavy rare earth elements (HREE) and shows pronounced negative Sr and moderate Eu anomalies, suggesting late-stage removal of plagioclase during magma evolution, thus pointing at fractional crystallization as an important petrogenetic process during differentiation from intermediate to silicic.

Table 1
Sample List and $\delta^{18}\text{O}$ Values of the Investigated Katla Rock Suite

Sample no.	Locality	Rock type	Composition	$\delta^{18}\text{O}$ (‰)	LOI
KAT-8	Rjúpnafell	Tephra	Basaltic	6.7	7.30
KAT01-A	Above Huldufjöll	Pumice	High-silica	4.3	3.43
KAT01-B	Above Huldufjöll	Obsidian	High-silica	4.1	0.15
KAT02-1	W. Húsárgil	Obsidian	High-silica	4.3	0.31
KAT02-2	W. Húsárgil	Pumice	High-silica	4.1	0.62
KAT02-3	W. Húsárgil	Tephra	Intermediate	4.6	3.12
KAT02-4	W. Húsárgil	Obsidian	High-silica	3.8	0.90
KAT02-5	W. Húsárgil	Pumice	High-silica	3.8	1.85
KAT02-7	E. Rjúpnagil	Basalt	Basaltic	5.8	−0.50
KAT02-8	E. Dalárgil	Bulk matrix	High-silica	2.7	2.29
KAT02-9b	E. Dalárgil	Pumice	High-silica	3.3	2.42
KAT02-10	E. Dalárgil	Pumice	High-silica	3.7	1.70
KAT02-11	W. Hofsárgil	Rhyolite	High-silica	3.7	1.43
KAT02-11 ^a	W. Hofsárgil	Rhyolite	Feldspar sep.	3.1	–
KAT02-12a	W. Hofsárgil	Basalt	Basaltic	5.8	−0.24
KAT02-12b	W. Hofsárgil	Pumice	High-silica	3.8	3.19
KAT02-12c	W. Hofsárgil	Bulk matrix	High-silica	3.4	2.25
KAT02-14	Dyrhólaey	Tephra	Intermediate	5.9	2.44
KAT02-17	Álftaver	Basalt	Basaltic	5.1	−0.26
KAT02-18	Austmannsbunga	Rhyolite	High-silica	6.4	0.32
KAT02-18 ^a	Austmannsbunga	Rhyolite	Feldspar sep.	6.3	–
KAT02-180 ^a	Austmannsbunga	Rhyolite	High-silica	6.4	0.30
KAT02-19a	Enta	Obsidian	High-silica	4.6	0.31
KAT02-19b	Enta	Pumice	High-silica	3.5	3.04
KAT02-20	Enta	Pumice	High-silica	4.0	0.70
KAT02-24	Dyrhólaey	Basalt	Basaltic	5.8	−0.02
KAT02-25	E. Rjúpnagil	Tephra	High-silica	2.9	2.08
KAT02-26	E. Rjúpnagil	Pumice	High-silica	4.3	1.45
KAT02-27a	E. Rjúpnagil	Obsidian	High-silica	3.6	0.29
KAT02-27b	E. Rjúpnagil	Pumice	High-silica	3.6	2.30
KAT02-28b	E. Rjúpnagil	Obsidian	High-silica	4.1	0.17
KAT02-37a	W. Húsárgil	Xenolith	High-silica	−3.3	0.22
KAT02-37b	W. Húsárgil	Xenolith	High-silica	−2.3	0.58
KAT02-37c	W. Húsárgil	Xenolith	High-silica	−3.6	0.59
KAT02-38b	W. Húsárgil	Obsidian	Intermediate	4.1	0.63
KAT02-39	W. Húsárgil	Pumice	High-silica	4.4	1.14
KAT02-40	Skógasandur	Lapilli	Basaltic	5.2	−0.64
KAT02-43	Sólheimajökull	Lapilli	Basaltic	5.9	−0.69
KAT02-44	E. Jokulsa	Lapilli	Basaltic	5.2	−0.47
KAT02-45	E. Húsárgil	Pumice	High-silica	3.8	0.21
KAT02-46 ^a	E. Húsárgil	Rhyolite	High-silica	4.0	0.29
KAT02-46 ^a	E. Húsárgil	Rhyolite	Feldspar sep.	3.2	–
KAT02-68	W. Mulakvisl	Lapilli	Basaltic	5.2	0.31

Table 1
Continued

Sample no.	Locality	Rock type	Composition	$\delta^{18}\text{O}$ (‰)	LOI
KAT-125	Atley	Tephra	Basaltic	4.3	−0.80
KAT-422	Atley	Tephra	Basaltic	8.5	8.00
KGV1A	Gvendarfell	Rhyolite	High-silica	4.2	0.74
KGV1A ^a	Gvendarfell	Rhyolite	Feldspar sep.	3.5	–
KGV1B ^a	Gvendarfell	Basalt	Basaltic	5.8	0.09
KGV3 ^a	Gvendarfell	Rhyolite	High-silica	3.8	0.13
KGV3 ^a	Gvendarfell	Rhyolite	Feldspar sep.	3.4	–
KGV4 ^a	Gvendarfell	Basalt	Basaltic	5.7	1.14
IC95-37	Thakgil	Granophyre	High-silica	−4.9	0.37
IC95-60	Austurgil	Obsidian	High-silica	5.0	0.07
IC95-65	Austurgil	Tephra	High-silica	4.8	2.93
IC95-66	Austurgil	Tuff	Basaltic	5.9	−0.70
IC95-67	Austurgil	Tuff	Basaltic	5.2	−0.55
IC95-132	Kriki	Obsidian	High-silica	4.2	0.15
IC95-139	Stórhryggur	Basalt	Basaltic	4.6	−0.69
IC95-142	Gvendarfell	Obsidian	High-silica	3.4	0.26
IC95-155	Oddnýjartjörn	Tephra	High-silica	3.1	3.06
IC95-193	Bláfell	Obsidian	High-silica	3.5	0.09
IC95-194	Bláfell	Tuff	Basaltic	6.1	−0.05

Note. Oxygen isotope values are given in δ -notation and presented in per mil (‰) relative to SMOW. The analytical error was 0.10‰ (1-sigma) for all samples of the study. Loss on ignition (LOI) values are given in wt.%. ^aOxygen isotope analysis from Budd (2015). LOI values are from Lacasse et al. (2007) and Budd (2015).

According to the published Sr and Nd isotopic data (Lacasse et al., 2007), the studied Katla samples show the lowest $^{143}\text{Nd}/^{144}\text{Nd}$ among reported Icelandic rocks (Figure 5), but there is considerable variation in $^{143}\text{Nd}/^{144}\text{Nd}$, which does not correlate with the degree of differentiation (see below). Instead, we observe distinct magmatic lineages with different $^{143}\text{Nd}/^{144}\text{Nd}$ and the variation in Nd isotopic composition likely reflects heterogeneity in the Katla mantle sources (see below). The relatively low $^{143}\text{Nd}/^{144}\text{Nd}$ values are compatible with, for example, a contribution from (recycled?) continental sources as suggested elsewhere (e.g., Torsvik et al., 2015). Importantly, if mantle source heterogeneity is a factor for explaining the variation in Nd isotopes, then we can test using oxygen isotopes if the possibly distinct mantle sources contain variable $\delta^{18}\text{O}$ signatures.

4. Methodology

Selected lava, xenolith, shallow intrusive, and tephra samples from the sample suites of Budd (2015) and Lacasse et al. (2007) were cut and thin section preparation was conducted. Back-scatter electron images (See Text S1 and Figure S2 in Supporting Information S1) were acquired on a Cameca SX100 electron microprobe at the University of Freiburg, Germany, under standard operating conditions of 15 kV accelerating voltage and 20 nA beam current.

In preparation for isotopic analysis, samples were crushed and powdered at Uppsala University and at the Natural History Museum in Stockholm using an agate mortar. No visible weathering was present in the analyzed samples. Whole-rock oxygen isotope analyses were carried out at the University of Cape Town (UCT), South Africa using conventional fluorination following the method by Vennemann and Smith (1990). A number of samples ($n = 10$) from a pilot investigation (Budd, 2015) were included in this study and were analyzed in the same laboratory, but are marked as being derived from the PhD thesis of D. Budd in the various tables. These include a limited number of data from feldspar separates ($n = 5$) analyzed by laser fluorination (LF) and the reader is referred to Budd (2015) for analytical details on the LF procedure. For the other samples, approximately 10 mg of bulk rock

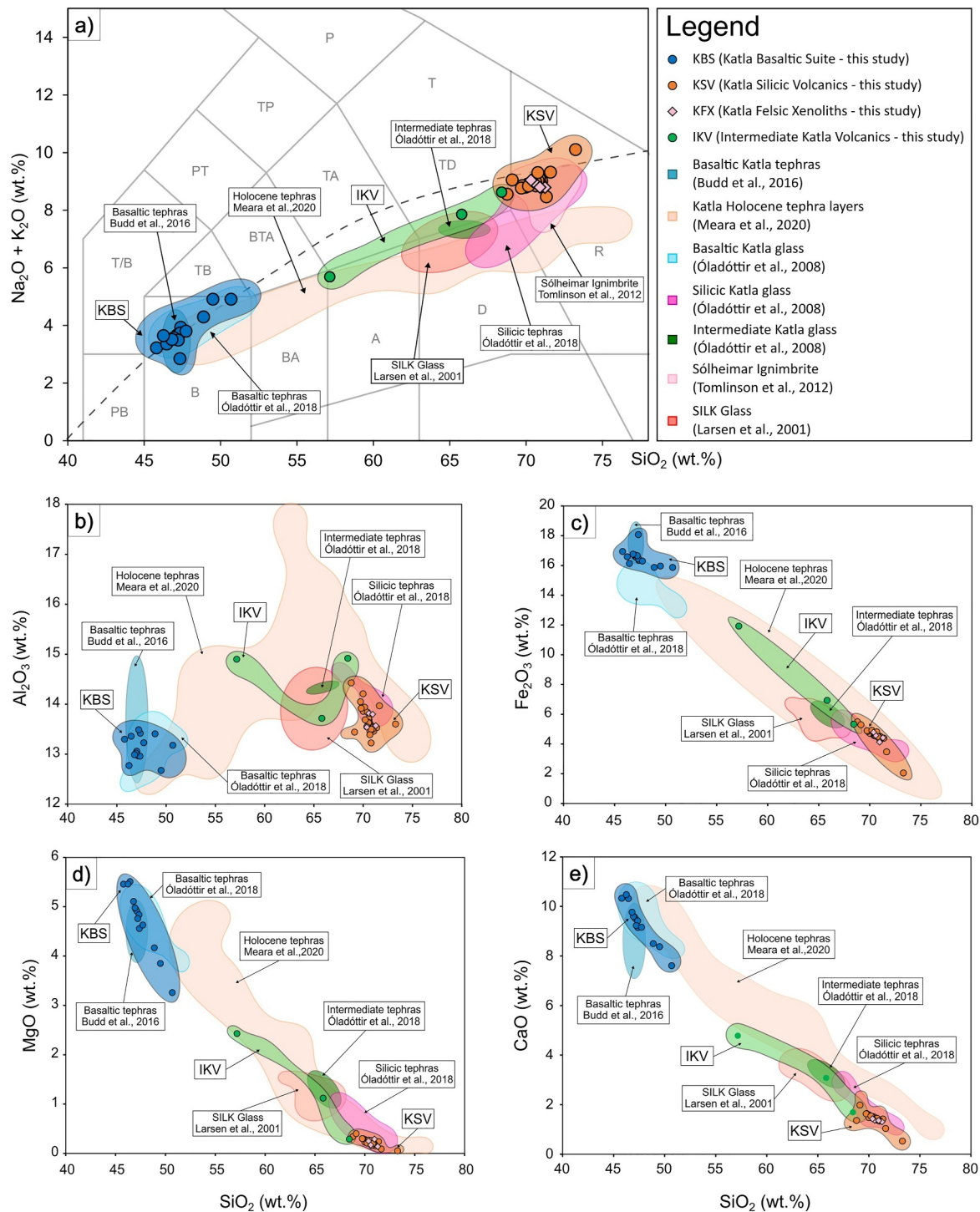


Figure 3. (a) Total alkali versus silica diagram (TAS) of whole-rock compositions for the Katla sample materials presented in this study using data from Budd (2015) and Lacasse et al. (2007). Available glass data in the literature are not plotted. The bimodality displayed for the Katla lavas of this study exhibits SiO_2 values between 43 and 51 wt.% for the basaltic suite and between 67 and 72 wt.% for the silicic suite. The silicic subset of samples ($n = 33$) is slightly alkaline to subalkaline and mainly plots in the rhyolite and the trachyte/trachydacite fields. The basaltic samples ($n = 17$) plot dominantly in the basalt field, but some samples are classified as picrobasalt. Intermediate compositions ($n = 3$) range between 56 and 66 wt.% and plot as basaltic andesite and trachyte/trachydacite. Literature reference data from Budd et al. (2016), Larsen et al. (2001), Meara et al. (2020), Óladóttir et al. (2008), Tomlinson et al. (2012). (b–e) Variation diagrams of whole-rock compositions versus SiO_2 of the Katla sample suite from Budd (2015) and Lacasse et al. (2007) (See Data Set S1 for full data set). (b) Al_2O_3 , (c) Fe_2O_3 , (d) MgO , (e) CaO versus SiO_2 wt.%. Literature reference fields as above. Note: a pronounced compositional gap exists between the Katla Silicic Volcanics and Katla Basaltic Suite. Abbreviations for (a) PB = picro-basalt, T/B = tephrite/basalt, PT = phono-tephrite, TP = tephry-phonolite, P = phonolite, TB = trachybasalt, BTA = basaltic trachyandesite, TA = trachyandesite, T = trachyte, TD = trachydacite, B = basalt, BA = basaltic andesite, A = andesite, D = dacite, and R = rhyolite.

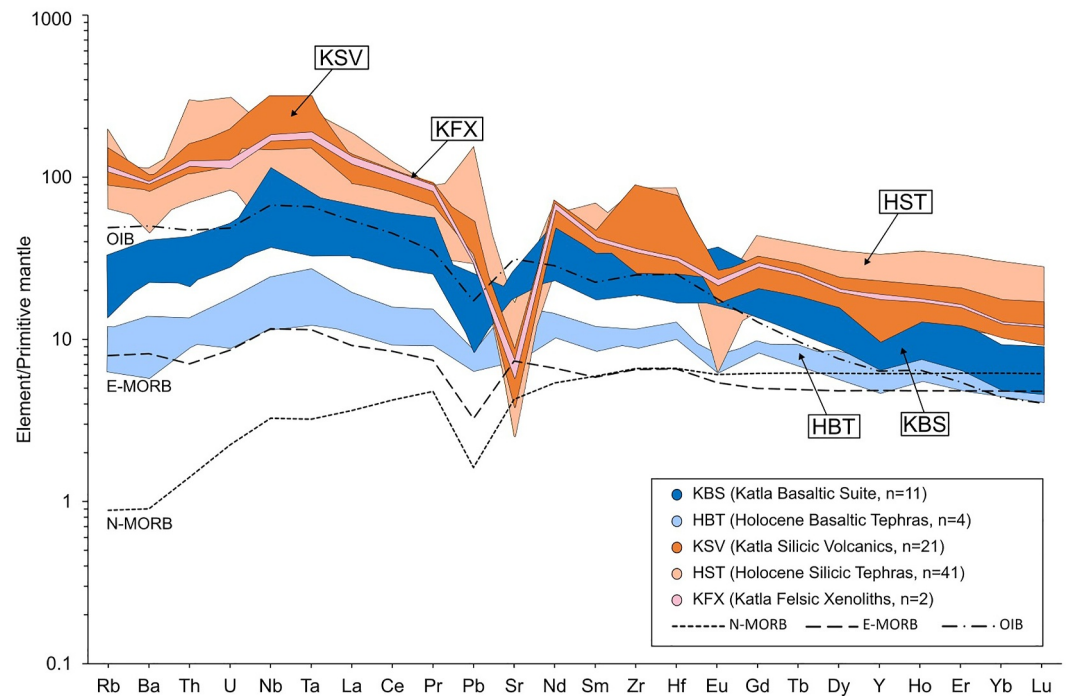


Figure 4. Multi-element variation diagram of available whole-rock Katla trace element compositions from Budd (2015) and Lacasse et al. (2007) (Data Set S1). Concentrations are normalized to primitive mantle from Sun and McDonough (1989). KBS ($n = 11$) displays enriched concentrations relative to E-MORB. The KSV ($n = 21$) displays an LREE enrichment as well as Sr and minor Eu depletions. Literature data (HST) from Meara et al. (2020) plotted for reference as well as average E-MORB and N-MORB after Sun and McDonough (1989).

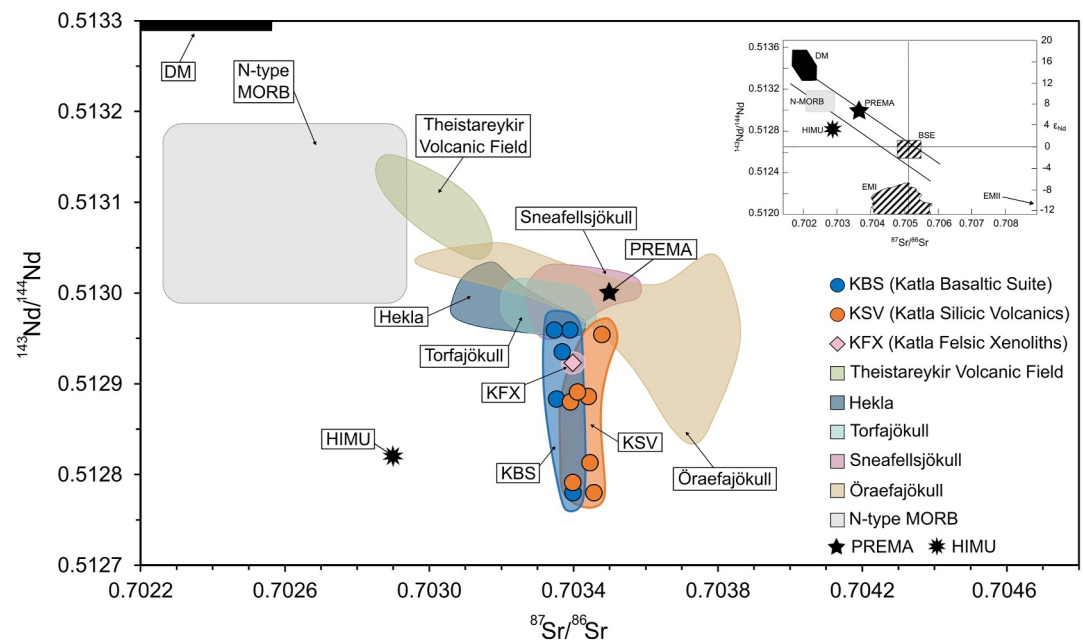


Figure 5. Sr and Nd isotope ratios of available KBS and KSV whole-rock samples (Lacasse et al., 2007; Data Set S1) compared to other volcanic rocks from Iceland (Hards et al., 2000; Kokfelt et al., 2006; Prestvik et al., 2001; Sigmarsson et al., 1992; Stecher et al., 1999) and HIMU, PREMA and DM reference values (Rollinson, 1993). Inset modified after Rollinson (1993).

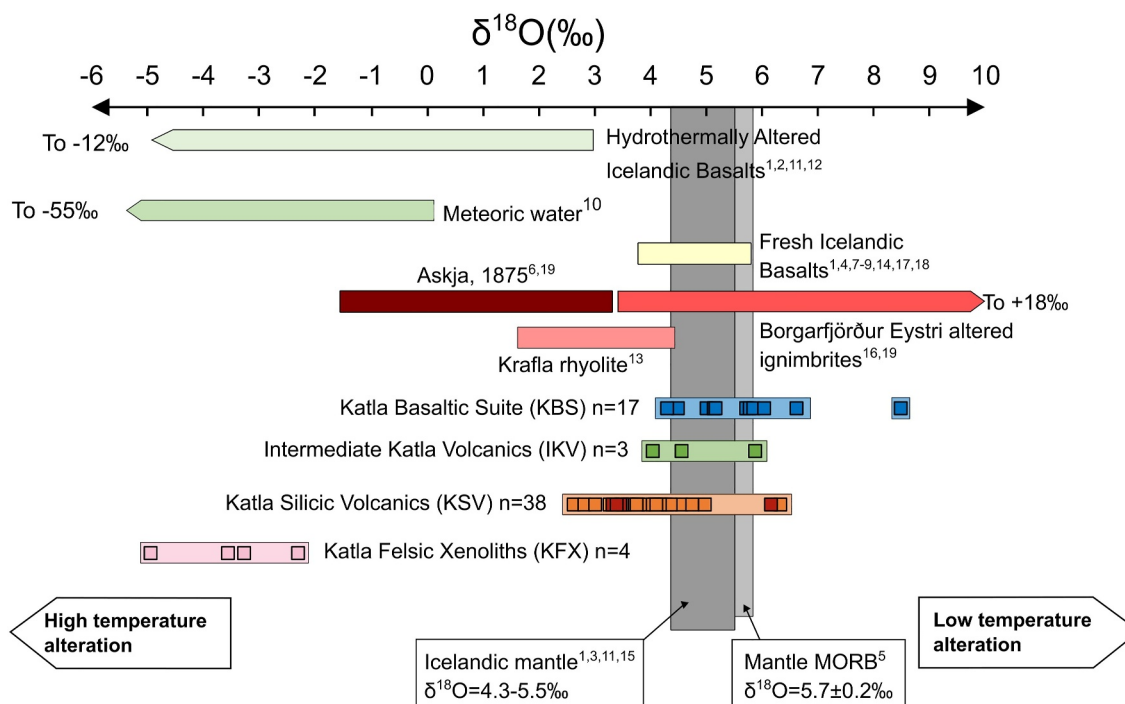


Figure 6. Whole-rock $\delta^{18}\text{O}$ values from this study and published Icelandic $\delta^{18}\text{O}$ reference values. The $\delta^{18}\text{O}$ range of the Katla Silicic Volcanics bulk rocks (KSV) ($n = 33$) falls between +2.7 and +6.4‰. Separated feldspar from silicic samples ($n = 5$) range between +3.1‰ and +6.3‰ and have been integrated into the KSV bar marked as dark red squares. The intermediate samples ($n = 3$) show a range of +4.1 to +5.9‰, and the Katla Basaltic Suite (KBS) ($n = 17$) falls between +4.3 and +8.5‰. The Katla Felsic Xenoliths (KFX) ($n = 4$), in turn, show values of -4.9 to -2.3‰. The $\delta^{18}\text{O}$ values of the silicic rocks show a range from mantle-like values to below the mantle MORB range, while the bulk of the basaltic rocks plot within the mantle MORB range. The felsic xenoliths show the lowest values in our Katla sample suite. Data from this study are plotted as squares, and the reference data are plotted as bars. Literature data from ¹Muehlenbachs et al. (1974); ²Hattori and Muehlenbachs (1982); ³Óskarsson et al. (1982); ⁴Condomines et al. (1983); ⁵Ito et al. (1987); ⁶Macdonald et al. (1987); ⁷Hemond et al. (1988); ⁸Sigmarsson et al. (1991); ⁹Macpherson et al. (2005); ¹⁰Valley et al. (2005); ¹¹Thirlwall et al. (2006); ¹²I. Bindeman et al. (2012); ¹³Pope et al. (2013); ¹⁴Budd (2015); ¹⁵Winpenny and MacLennan (2014); ¹⁶Berg et al. (2018); ¹⁷I. N. Bindeman et al. (2022); ¹⁸Troll et al. (2024); ¹⁹Martin and Sigmarsson (2010).

5. Oxygen Isotopic Composition of the Katla Rocks

Whole-rock $\delta^{18}\text{O}$ values (Table 1) of the Katla Basaltic Suite ($n = 17$) show a range between +4.3 and +8.5‰ and the bulk of the basaltic samples lie within the MORB range ($+5.7 \pm 0.2\text{‰}$; Cooper et al., 2009; Ito et al., 1987) and within the range of fresh Icelandic basalts (Figure 6). Two of the basaltic samples (KAT-8 and KAT-422) exhibit high $\delta^{18}\text{O}$ values (+6.7‰ and +8.5‰, respectively) but also distinctively high LOI values (>5 wt.%; Figure 7). Their oxygen isotopic compositions have likely been affected by hydrous alteration at very low temperatures (near the surface) (see Berg et al., 2018). We also suspect that the low $\delta^{18}\text{O}$ values (+4.3‰ and +4.6‰, respectively) of two basaltic samples (KAT-125 and IC95-139) with negative LOI may have been affected by post-solidification processes, such as reheating (cf. Berg et al., 2018; Donoghue et al., 2010; Figure 7), especially as these samples also have relatively low LOI values. Accordingly, we do not consider these extreme samples further since their $\delta^{18}\text{O}$ values may not be primary, that is, they may have been compromised by alteration or reheating processes. Thus, the most robust $\delta^{18}\text{O}$ values for the Katla basaltic rocks in our study range between +5.1 and +6.1‰.

The Katla Silicic Volcanics ($n = 33$) exhibit whole-rock $\delta^{18}\text{O}$ values ranging from +2.7‰ to +6.4‰, which is below or at the lower end of the range for typical mantle-derived Icelandic basaltic lavas (Figure 6), with the exception of two outliers with high $\delta^{18}\text{O}$ values of +6.4‰ (KAT02-18 and KAT02-180). Both of these samples show reasonable LOI (<1 wt.%; Figure 7) and we thus consider their $\delta^{18}\text{O}$ values to be magmatic. We also show data for feldspar separates for five samples. These have slightly lower values than their respective whole-rocks (by between 0.1 and 0.8‰), which is broadly consistent with equilibrium between the minerals and their host magma (Table 1).

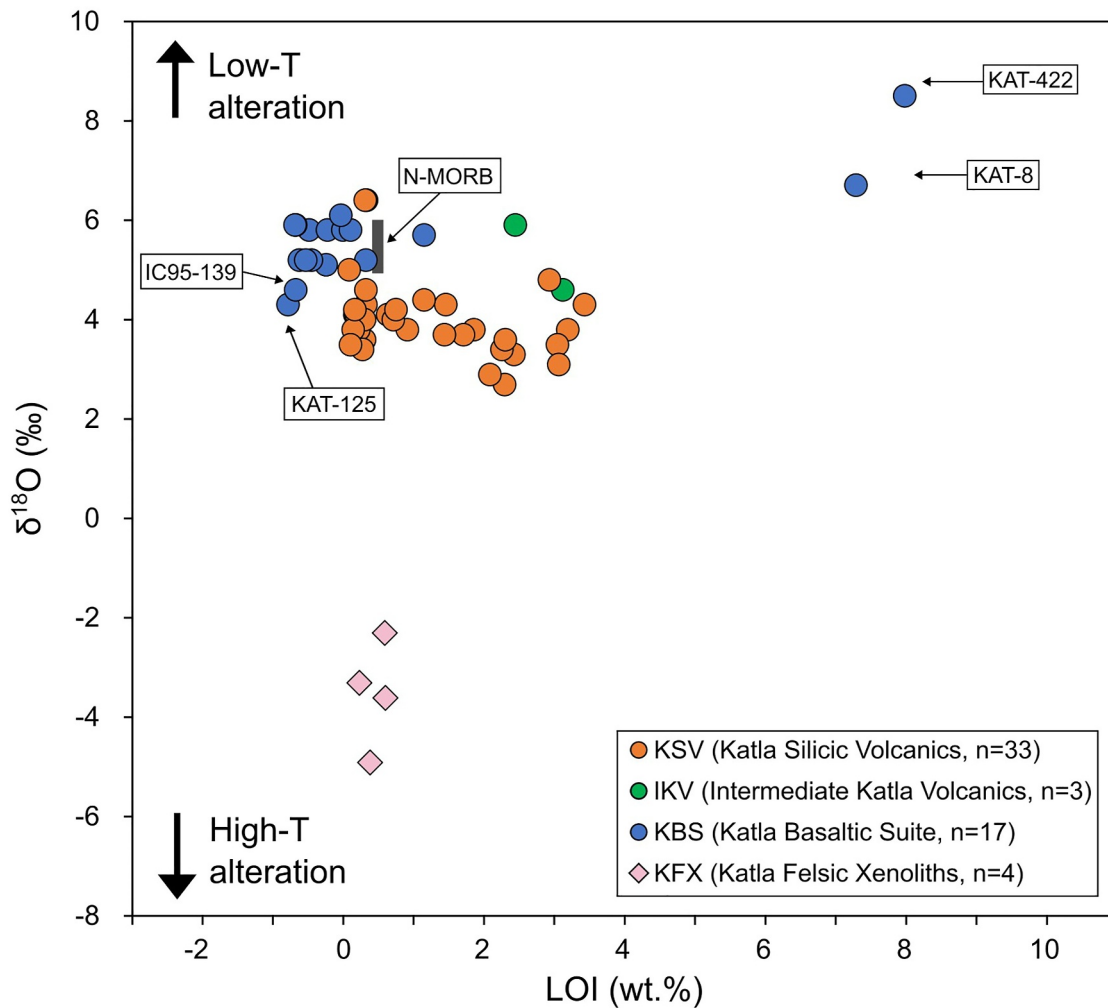


Figure 7. Whole-rock values for Loss on Ignition (LOI) versus oxygen isotope results. Uncertainty of the analyses is smaller than the symbol size. Arrows indicate directions of high- versus low-temperature alteration trends. A small number of basaltic samples have high LOI values that are associated with mildly to considerably elevated $\delta^{18}\text{O}$ values, whereas the majority of the KBS and the KSV as well as the Silicic xenoliths seem to show no significant within-group $\delta^{18}\text{O}$ variations with increases in LOI. The two high LOI samples are presumably hydrated and their oxygen isotope ratios are likely to reflect secondary processes rather than magmatic values.

The felsic xenoliths ($n = 4$) show strongly negative $\delta^{18}\text{O}$ values from -4.9 to -2.3‰ . We postulate that they experienced alteration through interaction with low- $\delta^{18}\text{O}$ meteoric waters in the upper crust before being captured by ascending magmas and partially remelted. The intermediate rock suite ($n = 3$) displays $\delta^{18}\text{O}$ values of $+4.1$ to $+5.9\text{‰}$, which is comparable with both the silicic and the basaltic suites. We consider these values to be magmatic although they may represent mixed values between basaltic and silica-rich endmember magmas.

In a plot of $^{143}\text{Nd}/^{144}\text{Nd}$ versus $\delta^{18}\text{O}$ values (Figure 8), the Katla volcanic rocks form three lineages that likely reflect Nd mantle source heterogeneity (see also Figure 5). However, $\delta^{18}\text{O}$ values do not correlate with $^{143}\text{Nd}/^{144}\text{Nd}$ and the basaltic samples show very similar $\delta^{18}\text{O}$ values, whereas the Silicic Volcanics show consistently lower $\delta^{18}\text{O}$ values compared to the Basaltic Suite. This strongly suggests that the variation in $\delta^{18}\text{O}$ value between basaltic and silica-rich volcanics is controlled by differentiation processes and not by mantle source heterogeneity. The differentiation processes, which are discussed in the following sections, were likely very similar within the distinct lineages.

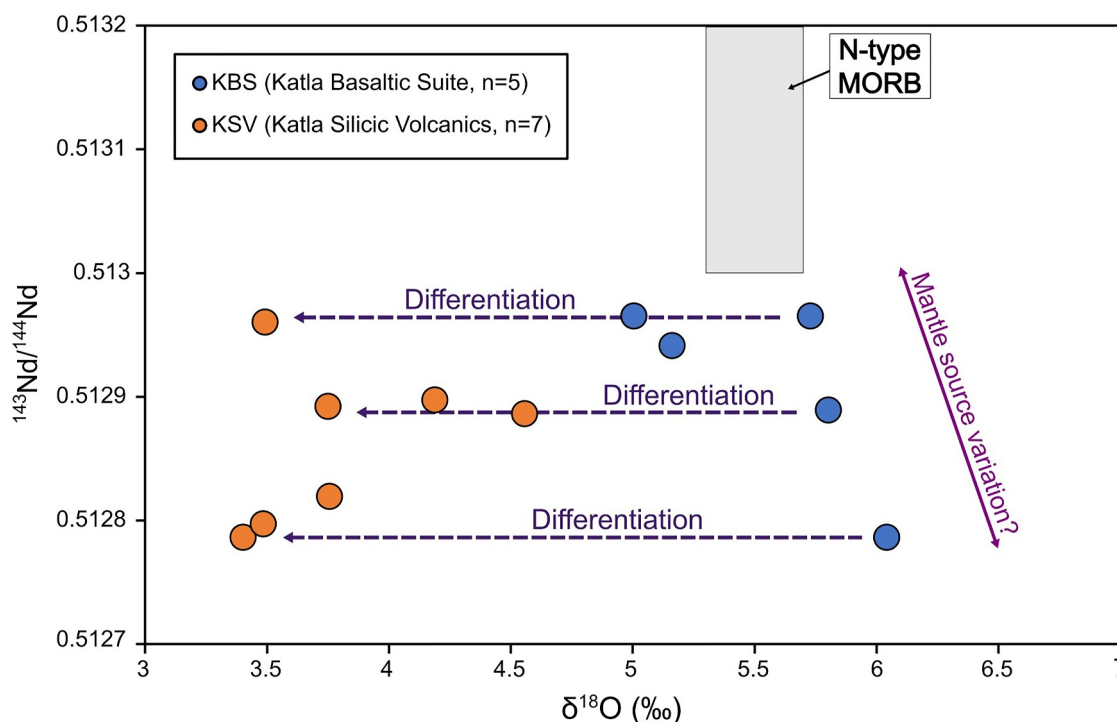


Figure 8. Whole-rock $\delta^{18}\text{O}$ values versus available $^{143}\text{Nd}/^{144}\text{Nd}$ of the Katla volcanic rocks. Nd isotopic values from Lacasse et al. (2007) distinguish several horizontal arrays on this plot. The uncertainty of the analyses is smaller than the symbol size. In detail, samples seem to form three distinct differentiation lineages (purple dashed arrows), the parental melts of which were either (i) derived from a source with possible minor variation in Nd isotopic composition or (ii) were variably affected by assimilation of for example, lower crustal materials.

6. Thermodynamic Modeling of Differentiation

The advanced energy-constrained modeling of closed- and open-system differentiation and its effects on phase equilibria, major elements, trace elements Zr and Sr, and $\delta^{18}\text{O}$ values was performed using MCS. The pressure of 100 MPa was chosen to represent the shallow magma chamber indicated beneath Katla, as explained earlier. The MCS versions used were 2019AH for major elements and 2019AM for trace elements and isotopes. The MELTS engine used for the calculations of phase equilibria was version 1.2.0 (Ghiorso & Gualda, 2015; Gualda et al., 2012).

An average of representative and non-altered samples of the Katla Basaltic Suite at liquidus temperature (1,125°C, as automatically defined by MELTS algorithms in MCS) was used as the magma starting composition (Data Set S2). A water content of 0.5 wt.% was assumed for the parental magma (see Budd et al., 2016). In the models involving assimilation, the average composition of the Felsic Xenoliths was used for the wall rock (assimilant) (Data Set S2). A value of 1 wt.% of water was used to represent moderate hydration of the wall rock due to hydrothermal alteration; this is higher than the water content of fresh Icelandic basalt (Radu et al., 2023), and also than the LOI in the (likely dehydrated) felsic xenoliths (Figure 7). The $\text{Fe}^{3+}/\text{Fe}^{\text{tot}}$ ratio was estimated to initially be 0.15 for the wall rock and the magma, but was not forced during the simulations (see Óskarsson et al., 1994).

We modeled assimilation by stopping-fractional crystallization (hereafter referred to as SFC_{MCS} ; Bohron et al., 2020) in which an assimilant is added to the crystallizing magma in bulk amounts using the recharge (R) function of MCS as controlled by the user. This can be broadly considered to simulate the assimilation of country rock material either as whole blocks of felsic wall rock or as portions of felsic partial melts from more mafic wall rock in the shallow crust. Hot (700°C) blocks of wall rock material were added to the fractionating magma in five steps, in which we varied the mass of the blocks between 1, 3, and 5 mass units (relative to the 100 mass units of the parental magma and resulting in total degrees of assimilation of 5, 15, and 25 wt.%, respectively). A hard stop temperature of 900°C was chosen for the models as this is sufficient to reach the most evolved compositions in the rock data.

For the behavior of trace elements Zr and Sr during crystallization, we used phase-specific partition coefficients based on Boudreau (1999), Ewart and Griffin (1994), Fujimaki (1986), Olin and Wolff (2010), Stimac and Hickmott (1994) (Data Set S2). The partition coefficients for olivine and apatite were constant, whereas the partition coefficients for feldspar (plagioclase), clinopyroxene, spinel, and rhomb-oxide were temperature-dependent. The treatment was based on the availability of temperature-dependent partition coefficient data and the overall stability range of the phases (see Heinonen et al., 2020).

The MCS trace element and isotope engine does not consider fractionation of $^{18}\text{O}/^{16}\text{O}$ during crystallization (see Heinonen et al., 2020). In order to take this effect into account, we modified the engine so that within each temperature step (= equilibrium crystallization step) oxygen isotopes in the magma were determined using equation $\Delta = (1/(F + \alpha(1 - F)) - 1) * 1000$, in which Δ is the change in $\delta^{18}\text{O}$ value, F is the fraction of the residual melt at the end of the temperature step (i.e., $1 -$ fraction of crystals formed), and α is $^{18}\text{O}/^{16}\text{O}$ in the formed crystals divided by $^{18}\text{O}/^{16}\text{O}$ in the residual melt. Phase-specific α values for a given temperature are poorly constrained (see Eiler, 2001) so instead we used a bulk value of 0.9995, which corresponds to circa +1 ‰ change in $\delta^{18}\text{O}$ from basaltic to rhyolitic compositions, which is commonly observed in magmatic systems controlled by fractionation (e.g., I. Bindeman, 2008; Chivas et al., 1982; Taylor & Sheppard, 1986).

The full major and trace element input and output for three SFC_{MCS} simulations and one FC_{MCS} simulation are compiled in Data Sets S3–S6 and selected results are illustrated in Figure 9. For more detailed information on how MCS works and on how to read the input and output information, the reader is referred to Bohrsen et al. (2020), Heinonen et al. (2020), and the MCS website (<https://mcs.geol.ucsb.edu/>). The pressure of 100 MPa was chosen on the basis of seismic evidence on the probable depth of the shallow magma chamber beneath Katla, but we also tested FC modeling at 500 MPa (depth of ~20 km). These results overlap with the FC curve illustrated in Figure 9 with a minor difference in initial Sr enrichment prior to plagioclase crystallization that was delayed by ~40°C in comparison to the 100 MPa model. Variations in pressure are thus neither expected to significantly influence the interpretations based on the presented results.

7. Discussion

7.1. Oxygen Isotopes and Differentiation of Katla Magmas

It is apparent from the modeling that fractional crystallization from basaltic parental magmas of the Katla Basaltic Suite cannot explain the low $\delta^{18}\text{O}$ values of the majority of the Katla Silicic Volcanics (Figure 9). Only two Katla Silicic Volcanics samples of this study (KAT02-18 and KAT02-180, trace element data only available for the former with $\delta^{18}\text{O} = +6.4\text{‰}$) could possibly originate from closed-system fractional crystallization from a Katla basaltic parent magma. These two samples fall, moreover, in line with similar silicic rocks from Hekla and Öraefajökull volcanoes with $\delta^{18}\text{O}$ values from +5.2 to +6.0‰, which were previously suggested to have originated from closed-system fractional crystallization processes (cf. I. Bindeman et al., 2012; Martin & Sigmarsson, 2007; Schattel et al., 2014; Sigmarsson et al., 1992). It is also possible that these samples are related to some older and completely different stages of volcanism in the area, since they have been collected from the caldera wall (Figure 2; see Lacasse et al., 2007). Apart from these two anomalous samples, the Katla Silicic Volcanics plot significantly below the predictions of the simple oxygen isotope fractionation model (cf. I. Bindeman, 2008; Figure 9). The observed elemental and isotope trends require open system processes and specifically the addition of a high-silica, low- $\delta^{18}\text{O}$ component by assimilation rather than interaction with low- $\delta^{18}\text{O}$ hydrothermal fluids during magma evolution. The latter process is unlikely since $\delta^{18}\text{O}$ values do not show a clear correlation with water content (i.e., with LOI) and elemental variations require assimilation of a wall rock of similar trace element concentrations to the silica-rich Katla volcanics (Figures 7 and 9). The best-fit results of the assimilation models correspond to a scenario in which hydrothermally altered crustal material represented by the Felsic Xenoliths are added to a fractionating magma represented by the Katla Basaltic Suite (Figure 9). Indeed, the full range of compositions from basalts to intermediate and felsic volcanics at Katla can be generated by a reasonable degree of assimilation between 5 and 25 wt.%.

The studied Felsic Xenoliths exhibit negative $\delta^{18}\text{O}$ values and display clear petrographic partial melting textures (see Figures S1e and S1f in Supporting Information S1), implying they were exposed to hydrothermal overprint and experienced subsequent recycling in hot Katla magmas during ascent. Most likely they represent part of the plutonic suite inside Katla. As previously argued by Gunnarsson et al. (1998), quenched xenoliths preserved at various degrees of remelting provide crucial support for the partial melting of older magmatic crust. The remelting

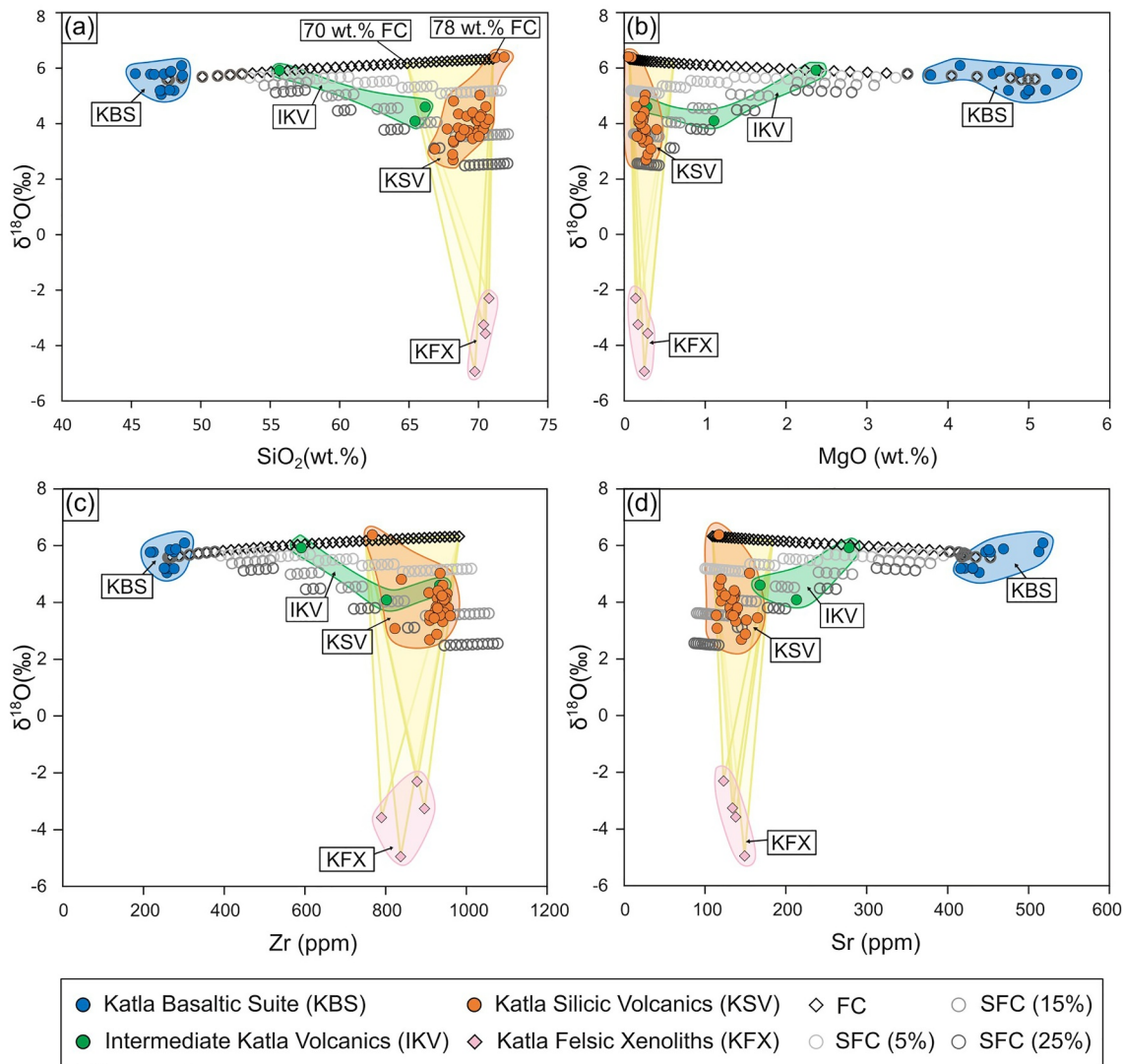


Figure 9. Whole-rock $\delta^{18}\text{O}$ values versus SiO_2 and MgO contents and Zr , and Sr concentrations of the Katla volcanic rocks and felsic xenoliths are shown together with the results of FC_{MCS} and SFC_{MCS} simulations (total of 5, 15, and 25 wt.% of assimilation in five stopping steps indicated by stepwise drops in $\delta^{18}\text{O}$ values). Major and trace elements plotted are from XRF analyses. Samples with a high LOI were excluded from this diagram. The yellow triangles illustrate bulk mixing of the felsic xenoliths with KBS-derived magma after 70–78 wt.% fractional crystallization. See text and Table 1 and Data Sets S3–S6 for model details.

of hydrothermally altered crustal material is potentially a very fast process as the material is hydrated, resulting in quick recycling of subvolcanic materials (cf. I. N. Bindeman & Simakin, 2014; Budd et al., 2017). The most likely source of low- $\delta^{18}\text{O}$ material is thus reasoned to be the hydrothermally altered roof and wall material of the magma reservoir as seen at other larger caldera systems such as the Yellowstone hotspot track, Toba volcano, and others (see Boroughs et al., 2012; Budd et al., 2017; Curtis et al., 2013; Pritchard & Larson, 2012; Riishuus et al., 2015; Seligman et al., 2014; Troch et al., 2019; Watts et al., 2012). In such systems, meteoric water altered the surrounding roof and wall rock at high temperatures because of extensive fracturing and brecciation caused by, for example, previous caldera collapses. Fractures act as pathways for the hydrothermal fluids and promote mobilization of the low- $\delta^{18}\text{O}$ material into the resident magma. A weakened and fractured reservoir roof is susceptible to partial collapse and stopping, for example, during earthquakes or minor magma injection events with rapid recycling and remelting of the low- $\delta^{18}\text{O}$ material (e.g., I. N. Bindeman & Simakin, 2014; Boroughs et al., 2012; Budd et al., 2017). In summary, our modeling, petrographic evidence, and comparison to volcanic systems elsewhere support the concept of edifice or crustal remelting rather than prolonged closed system fractional crystallization processes at work beneath Katla volcano. The Katla system therefore does not conform with either endmember of the volcanic system scheme in Iceland as proposed by Martin and Sigmarsson (2007). These

authors suggest that within rifts in Iceland, silicic magmas are generated mostly by partial melting of altered mafic crust, whereas in off-rift settings, silicic magmas are thought to form by fractional crystallization. Katla, located in the south domain of the East Volcanic Zone of Iceland, seems to reflect both partial melting and assimilation as well as fractional crystallization.

Is it possible to make a more comprehensive interpretation of the magma differentiation processes at Katla? First, it is important to acknowledge the bimodal distribution of rock compositions with only a few intermediate samples (Figure 3). The compositional gap is not straightforward to reconcile with a continuous AFC-style lineage, and several explanations may apply. The intermediate compositions may simply not be represented in the sample set as they may not have erupted and it is possible that magma compositions that were primitive (KBS) or had reached a certain degree of differentiation (KSV) were preferably tapped by the volcanic system. On the other hand, this may not be very likely since many ocean islands, and especially Iceland, are bimodal magmatic systems (e.g., Bunsen, 1851; Meyer et al., 1985; Sigmarsson et al., 1991; Sigurdsson, 1977). The intermediate compositions may then be the result of mixing of silica-rich magmas that contain a crustal anatectic component with mafic magmas that act as a heat source for the crustal melting (cf. Troll et al., 2004, 2021), mimicking an AFC-style evolution but circumventing a continuous crystallization series. A variation on this theme may be the PICA concept (progressively inhibited crustal assimilation), an explanation for the compositional gap proposed for the Carlingford Igneous Center, Ireland, where the crust can initially produce large volumes of silicic partial melts when heated by mafic magma before quickly becoming refractory (Meade et al., 2014). The resulting silicic magma ceases to be able to melt the surrounding crust as fertile partial melts are becoming rapidly exhausted and can no longer form (cf. Duffield & Ruiz, 1998; Meade et al., 2014). These melts can then only melt new crust if they encounter compositions with low melting points elsewhere in the magmatic system.

In addition, the distinct $\delta^{18}\text{O}$ values of the Katla Basaltic Suite versus the Katla Silicic Volcanics, coupled with the pronounced bimodal distribution for SiO_2 , MgO, Zr, and Sr concentrations (Figure 9), indicate that magmatic differentiation at Katla happens in two separate stages. The first stage consisted of fractionation (and possibly minor assimilation) deeper in the magma system, whereas the second stage consisted of bulk assimilation of felsic materials closer to the surface and closer in time to eruption. We do not have control of the possible assimilants in the first stage, but the involvement of an isotopically similar mafic country rock cannot be excluded. The suggested second stage of differentiation at shallow pressure is represented by the MCS models and subsequent bulk mixing lines between differentiated model compositions and the felsic xenoliths in Figure 9. The low- $\delta^{18}\text{O}$ assimilant represented by the Felsic Xenoliths had a very similar major, trace element, and radiogenic isotope composition to the KSV samples, but the original wall rock materials had been hydrated before being remelted. This similarity can explain the insignificant modification of most of the elemental and radiogenic isotope abundances (Figures 3–5), the latter within the different source lineages, but allows for significant changes in $\delta^{18}\text{O}$ values during the second stage (cf. I. N. Bindeman & Simakin, 2014; Figure 9).

We note that the results of a two-stage magma evolution process to produce the low- $\delta^{18}\text{O}$ Katla Silicic Volcanic suite are consistent with geophysical models of a deeper basaltic crustal magma storage system and a shallow (top few kilometer) reservoir (e.g., Jeddi et al., 2016; Figure 10). Such a broadly two-tiered arrangement in magma plumbing, with a shallow magma system in place, may have been a persistent feature for at least the last 8.5 kyrs (Budd et al., 2016). Geobarometry evidence from Budd (2015) and Budd et al. (2016) on silicic as well as basaltic compositions erupted over at least the last 8.5 kyrs indicates a shallow storage for silicic materials of around 3–5 km depth, whereas basaltic samples record magma storage depths down to upper mantle levels at >25 km, but with marked peaks at of 10–15 km depth, at 20–25 km depth, and again at 30 km depth beneath the volcano. This is broadly in line with recent OPAM glass barometry published by Baxter et al. (2023), who suggest that Katla magmas last equilibrated in the top 3–5 km, which is in line with the upper end of the seismic anomaly described by Jeddi et al. (2016), and which these authors interpreted as an upper (silicic) magma reservoir system under Katla volcano.

Finally, we emphasize that regardless of the differentiation taking place in one or several stages, our models strongly suggest that the low $\delta^{18}\text{O}$ values of the Katla Silicic Volcanics are the result of assimilation of older hydrothermally altered crust and are not inherited from the mantle source.

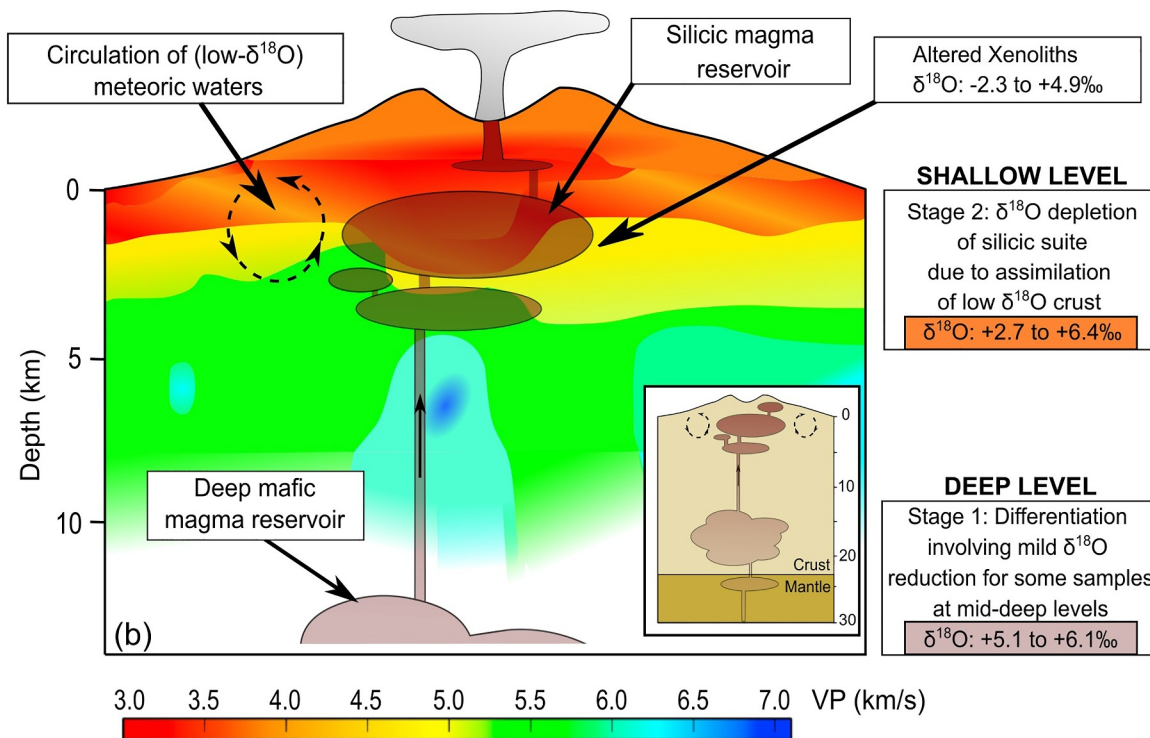
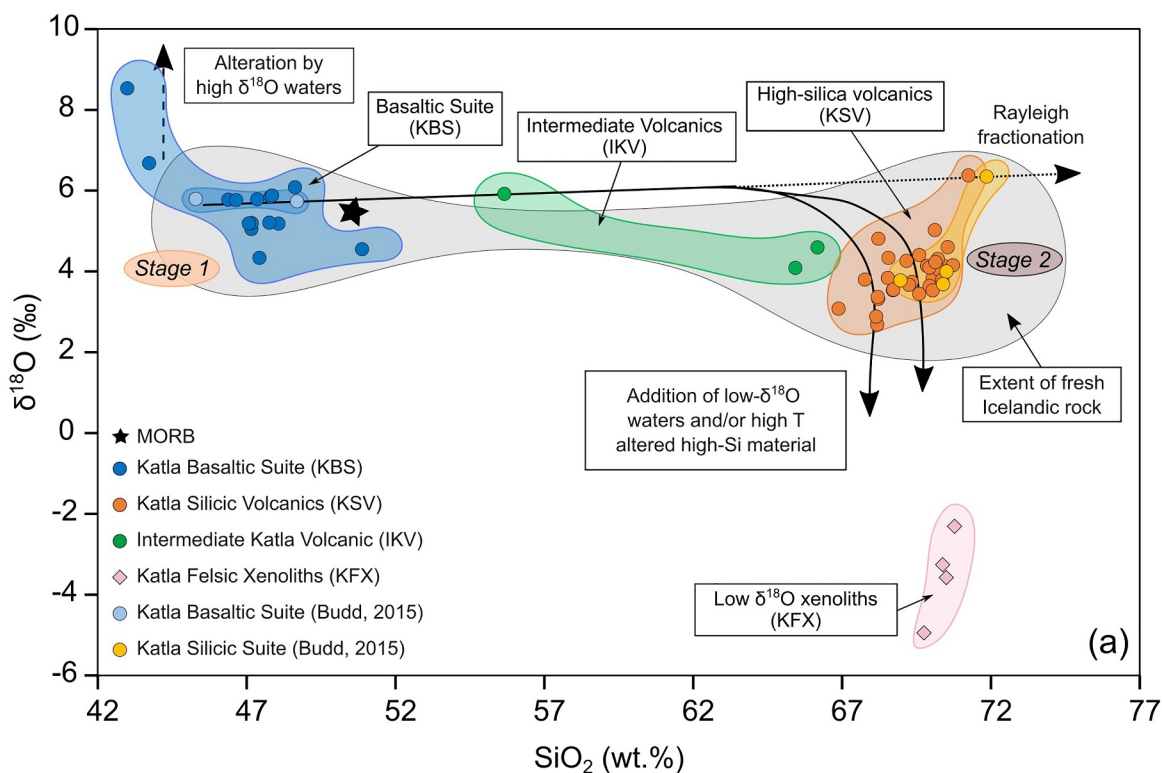


Figure 10.

7.2. Implications for Iceland Magma Genesis

In a wider context, AFC-style processes and assimilation of partial or bulk melts of hydrothermally altered crust may help explain the relatively high abundance of silicic magmatism in Iceland compared to MORB and ocean island volcanic settings. Low- $\delta^{18}\text{O}$ silicic rocks similar to Katla Silicic Volcanics have been described from several central volcanoes and caldera-type localities such as Askja ($\delta^{18}\text{O} = -9.0$ to $+2.8\%$) and Krafla ($\delta^{18}\text{O} = +3.1\%$) and many other high-silica low- $\delta^{18}\text{O}$ magmatic centers in Iceland (e.g., I. Bindeman, 2008; I. Bindeman et al., 2012; Gurenko et al., 2015; Macdonald et al., 1987; Pope et al., 2013; Zierenberg et al., 2013). In addition, xenoliths of felsic composition are common in Icelandic eruptive material (Gurenko et al., 2015; Sigurdsson, 1968). Previously, Walker (1966) suggested that fractional crystallization alone could not account for the high abundance of silicic compositions with the simultaneous absence of intermediate compositions in Iceland, because closed-system FC would produce only ~ 5 wt.% high-silica rhyolite. Iceland is an excellent natural laboratory to study these kinds of processes since the northerly position and the cold oceanic climate promote deep meteoric-hydrothermal systems with low $\delta^{18}\text{O}$ values (Troch et al., 2019), which makes the assimilation process traceable using oxygen isotopes. In subtropical and tropical oceanic islands this might be more difficult, yet we encourage research on whether open-system processes described here and elsewhere could explain bimodal compositions on other oceanic islands as well (e.g., Bohron & Reid, 1997). Potential contributions from not only felsic but also pre-existing mafic crust remain to be studied in detail in Katla and elsewhere.

The digestion of earlier crust may not only explain the bimodal distribution of volcanic rock compositions but also contribute to the style of the eruptions. Assimilation processes have been suggested to influence the eruptive behavior of many volcanic systems, especially by increasing the volatile budgets of magmas (e.g., Borisova et al., 2013; Budd et al., 2017; Gardner et al., 2013; Handley et al., 2018, Takach et al., 2024). This notion is consistent with the relatively low LOI of the felsic xenoliths compared to the LOI of the silicic samples at the same SiO_2 contents (see Figure 7), implying that they released volatiles during heating and remelting (e.g., Donoghue et al., 2010). The possible late and large-scale assimilation stage of hydrothermally altered crust, as described here for Katla, has the potential to introduce considerable amounts of volatiles in already differentiated magma compositions. The addition of volatiles enhances exsolution of a fluid phase at higher pressures and decreases density of magmas, and can thus promote tapping and eruption of felsic compositions in magmatic systems, especially as some recent studies have suggested that there is a sweet spot for eruptive behavior at about ~ 4 – 5.5 wt.% of dissolved water contents (Brookfield et al., 2023; Popa et al., 2021). Such high water contents might be difficult to reach only by fractionation of rather volatile-poor primitive magmas in oceanic island settings and we speculate that crustal assimilation may play an important but perhaps underrated role in driving explosive behavior at more evolved ocean island volcanoes.

8. Conclusions

To advance the debate on the origin of silica-rich rocks in Iceland, this study contributes over 60 new oxygen isotope values on a suite of basaltic to silica-rich rocks from Katla volcano. The $\delta^{18}\text{O}$ values of the basaltic sample suite (46–50 wt. % SiO_2) range from $+4.3$ to $+8.5\%$, and the intermediate suite ranges between $+4.1$ and $+5.9\%$,

Figure 10. (a) Summary SiO_2 versus $\delta^{18}\text{O}$ plot of the new Katla oxygen data presented here compared with previously reported “fresh” Icelandic rocks (gray cloud; I. N. Bindeman et al., 2022; Condomines et al., 1983; Gunnarsson et al., 1998; Hards et al., 2000; Hemond et al., 1988; Macpherson et al., 2005; Prestvik et al., 2001; Sigmarsson et al., 1992; Troll et al., 2024). The dominant fraction of the analyzed samples falls within the previously established Icelandic rock array with only very few exceptions. A Rayleigh fractionation curve (dotted black line) from one of the basaltic (parent) samples outlines the effects of closed-system crystal fractionation from basalt to rhyolite, which results in a $\sim 1\%$ increase (e.g., I. Bindeman, 2008; Taylor & Sheppard, 1986). The bulk of the silicic Katla samples display a distinct deviation from the closed-system fractionation curve showing a trend toward lower $\delta^{18}\text{O}$ values. This implies the addition of low- $\delta^{18}\text{O}$ material during magmatic evolution (schematically represented by solid black lines), likely with a component similar to the partially melted silicic xenoliths of this study as they display sufficiently low $\delta^{18}\text{O}$ values. (b) Schematic sketch of the plumbing system beneath the Katla caldera. A shallow level magma reservoir has recently been imaged through a P-wave velocity model, as shown in the color scheme at the bottom of the figure (after Jeddi et al., 2016). From these geophysical constraints (Jeddi et al., 2016), a high velocity core at 5 km depth and below is interpreted to consist of mafic cumulates, above which hot rhyolitic material is proposed to reside. We show the broadly two-tiered magma plumbing system on the basis of geophysical and geobarometry studies (cf. Budd, 2015; Budd et al., 2016; Jeddi et al., 2016, 2017) with a set of shallow reservoirs (at 5–2 km depth) rather than a single larger shallow-level chamber. We postulate that magma evolution takes place initially in a deep- to mid-crustal mafic magma reservoir system, followed by differentiation and interaction with hydrated sub-volcanic wall and roof rock (with lower $\delta^{18}\text{O}$ values) in a shallow-level silicic magma reservoir. This second-stage of differentiation at shallow crustal levels causes a decrease in $\delta^{18}\text{O}$ values in the evolved silicic magmas but does not cause significant changes in major or trace elements at that stage since the wall rock materials are otherwise similar to the silicic magmas hosted in the shallow system. The low $\delta^{18}\text{O}$ values of the wall- and country rock and thus the assimilants are the result of circulation of meteoric waters that are characterized by variably depleted $\delta^{18}\text{O}$ values.

but when eliminating altered samples, the basaltic suite ranges from 5.1 to 6.1‰, showing a narrow compositional field that overlaps with MORB (5.5–5.7‰; Cooper et al., 2009; Ito et al., 1987). The $\delta^{18}\text{O}$ values of the Katla silicic volcanic rocks (67 to >70 wt.% SiO_2), in turn, range between +2.7 and +6.4‰, whereas the silicic xenoliths range between –4.9 and –2.3‰. Approximately 97% of the analyzed silicic rocks at Katla thus show low- $\delta^{18}\text{O}$ values (≤ 5.0 ‰), and are thus significantly below the $\delta^{18}\text{O}$ values of the mantle MORB range. We postulate a distinct two-stage magma evolution process to produce the low- $\delta^{18}\text{O}$ silicic rocks at Katla. The first stage involves basaltic magmas with “normal” upper mantle type oxygen isotope ratios (cf. I. N. Bindeman et al., 2022) that begin to fractionate to more silica rich compositions. In the second stage, the evolving magmas ascend and interact with low- $\delta^{18}\text{O}$ sub-volcanic and/or plutonic material of the hydrated magma chamber walls and roof at shallow crustal depths. The major finding of this work, the two-stage magma evolution process that explains the presented geochemical data, is further supported by existing geobarometry and geophysical studies at Katla, supporting a deeper basaltic magma reservoir system (>10 km) that feeds a silicic magma domain in the upper crust (c. 3 km). This conceptual model is further supported by partial melting textures (symplectites) and resorption features in the felsic xenoliths that also show the lowest $\delta^{18}\text{O}$ values recorded in the entire Katla sample suite, and which can be shown to be an appropriate assimilated through energy constrained geochemical modeling. Importantly, our data underline that the “low $\delta^{18}\text{O}$ signature” in Katla silicic volcanics is a feature added to the magmas during crustal differentiation and does not constitute evidence for unusually low $\delta^{18}\text{O}$ mantle under southeast Iceland.

Data Availability Statement

The data underlying this study is available in Troll et al. (2025) [Dataset]. The data set includes whole rock data and modeling parameters. The MCS modeling was performed using the Magma Chamber Simulator (MCS) software package available from the UC Santa Barbara website (<https://mcs.geol.ucsb.edu/code>).

Acknowledgments

We are grateful to Renaud Merle for helping with sample preparation at NRM Stockholm. David Budd is acknowledged for discussion during the early stages of this work and encouragement to integrate unpublished data from his PhD thesis into the current study. We also thank Julia Neukampf and an anonymous reviewer for constructive feedback and Dimitra Antoniou and Monika Hawrylak for help with the preparation of the manuscript and display materials. VRT and FMD acknowledge financial support by the Science Foundation Sweden (Grant 2020-03789) and by ERC project ‘ROTTnROCK’, a research project funded by the European Research Council under the European Union’s Horizon Europe Programme/ERC synergy Grant [ERC-2023-SyG 101118491].

References

- Baxter, R. J. M., MacLennan, J., Neave, D. A., & Thordarson, T. (2023). Depth of magma storage under Iceland controlled by magma fluxes. *Geochemistry, Geophysics, Geosystems*, 24(7), e2022GC010811. <https://doi.org/10.1029/2022GC010811>
- Berg, S. E., Troll, V. R., Harris, C., Deegan, F. M., Riishuus, M. S., Burchardt, S., & Krumbholz, M. (2018). Exceptionally high whole-rock $\delta^{18}\text{O}$ values in intra-caldera rhyolites from Northeast Iceland. *Mineralogical Magazine*, 82(5), 1147–1168. <https://doi.org/10.1180/mgm.2018.114>
- Bindeman, I. (2008). Oxygen Isotopes in Mantle and Crustal Magmas as Revealed by Single Crystal Analysis. *Reviews in Mineralogy and Geochemistry*, 69(1), 445–478. <https://doi.org/10.2138/rmg.2008.69.12>
- Bindeman, I., Gurenko, A., Carley, T., Miller, C., Martin, E., & Sigmarsson, O. (2012). Silicic magma petrogenesis in Iceland by remelting of hydrothermally altered crust based on oxygen isotope diversity and disequilibria between zircon and magma with implications for MORB. *Terra Nova*, 24(3), 227–232. <https://doi.org/10.1111/j.1365-3121.2012.01058.x>
- Bindeman, I., Gurenko, A., Sigmarsson, O., & Chaussidon, M. (2008). Oxygen isotope heterogeneity and disequilibria of olivine crystals in large volume Holocene basalts from Iceland: Evidence for magmatic digestion and erosion of Pleistocene hyaloclastites. *Geochimica et Cosmochimica Acta*, 72(17), 4397–4420. <https://doi.org/10.1016/j.gca.2008.06.010>
- Bindeman, I. N., Deegan, F. M., Troll, V. R., Thordarson, T., Höskuldsson, Á., Moreland, W. M., et al. (2022). Diverse mantle components with invariant oxygen isotopes in the 2021 Fagradalsfjall eruption, Iceland. *Nature Communications*, 13(1), 3737. <https://doi.org/10.1038/s41467-022-31348-7>
- Bindeman, I. N., & Simakin, A. G. (2014). Rhyolites—Hard to produce, but easy to recycle and sequester: Integrating microgeochemical observations and numerical models. *Geosphere*, 10(5), 930–957. <https://doi.org/10.1130/GES00969.1>
- Björnsson, H., Pálsson, F., & Gudmundsson, M. T. (2000). Surface and bedrock topography of the Mýrdalsjökull ice cap, Iceland: The Katla caldera, eruption sites and routes of Jökulhlaups. *Jökull Journal*, 49, 29–46. <https://doi.org/10.33799/jokull2000.49.029>
- Blake, S. (1984). Magma mixing and hybridization processes at the alkalic, silicic, Torfajökull central volcano triggered by tholeiitic Veidivötn fissuring, south Iceland. *Journal of Volcanology and Geothermal Research*, 22(1–2), 1–31. [https://doi.org/10.1016/0377-0273\(84\)90033-7](https://doi.org/10.1016/0377-0273(84)90033-7)
- Blockley, S. P. E., Lane, C. S., Lotter, A. F., & Pollard, A. M. (2007). Evidence for the presence of the Vedde Ash in Central Europe. *Quaternary Science Reviews*, 26(25–28), 3030–3036. <https://doi.org/10.1016/j.quascirev.2007.09.010>
- Bohrson, W. A., & Reid, M. R. (1997). Genesis of Silicic Peralkaline Volcanic Rocks in an Ocean Island Setting by Crustal Melting and Open-system Processes: Socorro Island, Mexico. *Journal of Petrology*, 38(9), 1137–1166. <https://doi.org/10.1093/ptro/38.9.1137>
- Bohrson, W. A., Spera, F. J., Ghiorsio, M. S., Brown, G. A., Creamer, J. B., & Mayfield, A. (2014). Thermodynamic Model for Energy-Constrained Open-System Evolution of Crustal Magma Bodies Undergoing Simultaneous Recharge, Assimilation and Crystallization: The Magma Chamber Simulator. *Journal of Petrology*, 55(9), 1685–1717. <https://doi.org/10.1093/ptro/legu036>
- Bohrson, W. A., Spera, F. J., Heinonen, J. S., Brown, G. A., Scruggs, M. A., Adams, J. V., et al. (2020). Diagnosing open-system magmatic processes using the Magma Chamber Simulator (MCS): Part I—Major elements and phase equilibria. *Contributions to Mineralogy and Petrology*, 175(11), 104. <https://doi.org/10.1007/s00410-020-01722-z>
- Borisova, A. Y., Martel, C., Gouy, S., Pratomo, I., Sumarti, S., Toutain, J.-P., et al. (2013). Highly explosive 2010 Merapi eruption: Evidence for shallow-level crustal assimilation and hybrid fluid. *Journal of Volcanology and Geothermal Research*, 261, 193–208. <https://doi.org/10.1016/j.jvolgeores.2012.11.002>
- Borouh, S., Wolff, J. A., Ellis, B. S., Bonnicksen, B., & Larson, P. B. (2012). Evaluation of models for the origin of Miocene low- $\delta^{18}\text{O}$ rhyolites of the Yellowstone/Columbia River Large Igneous Province. *Earth and Planetary Science Letters*, 313–314, 45–55. <https://doi.org/10.1016/j.epsl.2011.10.039>

- Boudreau, A. E. (1999). PELE—A version of the MELTS software program for the PC platform. *Computers & Geosciences*, 25(2), 201–203. [https://doi.org/10.1016/S0098-3004\(98\)00117-4](https://doi.org/10.1016/S0098-3004(98)00117-4)
- Brookfield, A., Cassidy, M., Weber, G., Popa, R.-G., Bachmann, O., & Stock, M. J. (2023). Magmatic volatile content and the overpressure “sweet spot”: Implications for volcanic eruption triggering and style. *Journal of Volcanology and Geothermal Research*, 444, 107916. <https://doi.org/10.1016/j.jvolgeores.2023.107916>
- Budd, D. A. (2015). *Characterising volcanic magma plumbing systems: A tool to improve eruption forecasting at hazardous volcanoes* (Doctoral dissertation, Uppsala University). Acta Universitatis Upsaliensis.
- Budd, D. A., Troll, V. R., Dahren, B., & Burchardt, S. (2016). Persistent multitiered magma plumbing beneath Katla volcano, Iceland. *Geochemistry, Geophysics, Geosystems*, 17(3), 966–980. <https://doi.org/10.1002/2015GC006118>
- Budd, D. A., Troll, V. R., Deegan, F. M., Jolis, E. M., Smith, V. C., Whitehouse, M. J., et al. (2017). Magma reservoir dynamics at Toba caldera, Indonesia, recorded by oxygen isotope zoning in quartz. *Scientific Reports*, 7(1), 40624. <https://doi.org/10.1038/srep40624>
- Bunsen, R. (1851). Über die prozesse der vulkanischen Gesteinbildungen Island. *Annalen der Physik und Chemie*, 159(6), 197–272. <https://doi.org/10.1002/andp.18511590602>
- Carmichael, I. S. E. (1964). The Petrology of Thingmuli, a Tertiary Volcano in Eastern Iceland. *Journal of Petrology*, 5(3), 435–460. <https://doi.org/10.1093/ptrology/5.3.435>
- Charretre, G., Tegner, C., & Haase, K. (2013). Multiple ways of producing intermediate and silicic rocks within Thingmúli and other Icelandic volcanoes. *Contributions to Mineralogy and Petrology*, 166(2), 471–490. <https://doi.org/10.1007/s00410-013-0886-1>
- Chivas, A. R., Andrew, A. S., Sinha, A. K., & O’Neil, J. R. (1982). Geochemistry of a Pliocene–Pleistocene oceanic-arc plutonic complex, Guadalcanal. *Nature*, 300(5888), 139–143. <https://doi.org/10.1038/300139a0>
- Condomines, M., Grönvold, K., Hooker, P. J., Muehlenbachs, K., O’Nions, R. K., Óskarsson, N., & Oxburgh, E. R. (1983). Helium, oxygen, strontium and neodymium isotopic relationships in Icelandic volcanics. *Earth and Planetary Science Letters*, 66, 125–136. [https://doi.org/10.1016/0012-821X\(83\)90131-0](https://doi.org/10.1016/0012-821X(83)90131-0)
- Cooper, K. M., Eiler, J. M., Sims, K. W. W., & Langmuir, C. H. (2009). Distribution of recycled crust within the upper mantle: Insights from the oxygen isotope composition of MORB from the Australian–Antarctic Discordance. *Geochemistry, Geophysics, Geosystems*, 10(12), Q12004. <https://doi.org/10.1029/2009GC002728>
- Curtis, C. G., Harris, C., Trumbull, R. B., De Beer, C., & Mudzanani, L. (2013). Oxygen Isotope Diversity in the Anorogenic Koegel Fontein Complex of South Africa: A Case for Basement Control and Selective Melting for the Production of Low- $\delta^{18}\text{O}$ Magmas. *Journal of Petrology*, 54(7), 1259–1283. <https://doi.org/10.1093/ptrology/egt011>
- DePaolo, D. J. (1981). Trace element and isotopic effects of combined wallrock assimilation and fractional crystallization. *Earth and Planetary Science Letters*, 53(2), 189–202. [https://doi.org/10.1016/0012-821X\(81\)90153-9](https://doi.org/10.1016/0012-821X(81)90153-9)
- Donoghue, E., Troll, V. R., & Harris, C. (2010). Fluid–Rock Interaction in the Miocene, Post-Caldera, Tejada Intrusive Complex, Gran Canaria (Canary Islands): Insights from Mineralogy, and O- and H-Isotope Geochemistry. *Journal of Petrology*, 51(10), 2149–2176. <https://doi.org/10.1093/ptrology/egq052>
- Duffield, W. A., & Ruiz, J. (1998). A model that helps explain Sr-isotope disequilibrium between feldspar phenocrysts and melt in large-volume silicic magma systems. *Journal of Volcanology and Geothermal Research*, 87(1–4), 7–13. [https://doi.org/10.1016/S0377-0273\(98\)00071-7](https://doi.org/10.1016/S0377-0273(98)00071-7)
- Eiler, J. M. (2001). Oxygen Isotope Variations of Basaltic Lavas and Upper Mantle Rocks. *Reviews in Mineralogy and Geochemistry*, 43(1), 319–364. <https://doi.org/10.2138/gsrmg.43.1.319>
- Ewart, A., & Griffin, W. L. (1994). Application of proton-microprobe data to trace-element partitioning in volcanic rocks. *Chemical Geology*, 117(1–4), 251–284. [https://doi.org/10.1016/0009-2541\(94\)90131-7](https://doi.org/10.1016/0009-2541(94)90131-7)
- Fujimaki, H. (1986). Partition coefficients of Hf, Zr, and REE between zircon, apatite, and liquid. *Contributions to Mineralogy and Petrology*, 94(1), 42–45. <https://doi.org/10.1007/BF00371224>
- Furman, T., Frey, F. A., & Meyer, P. S. (1992). Petrogenesis of Evolved Basalts and Rhyolites at Austurhorn, Southeastern Iceland: The Role of Fractional Crystallization. *Journal of Petrology*, 33(6), 1405–1445. <https://doi.org/10.1093/ptrology/33.6.1405>
- Gardner, M. F., Troll, V. R., Gamble, J. A., Gertisser, R., Hart, G. L., Ellam, R. M., et al. (2013). Crustal Differentiation Processes at Krakatau Volcano, Indonesia. *Journal of Petrology*, 54(1), 149–182. <https://doi.org/10.1093/ptrology/egs066>
- Geiger, H., Mattsson, T., Deegan, F. M., Troll, V. R., Burchardt, S., Gudmundsson, Ó., et al. (2016). Magma plumbing for the 2014–2015 Holuhraun eruption, Iceland. *Geochemistry, Geophysics, Geosystems*, 17(8), 2953–2968. <https://doi.org/10.1002/2016GC006317>
- Ghiorso, M. S., & Gualda, G. A. R. (2015). An H₂O–CO₂ mixed fluid saturation model compatible with rhyolite-MELTS. *Contributions to Mineralogy and Petrology*, 169(6), 53. <https://doi.org/10.1007/s00410-015-1141-8>
- Gualda, G. A. R., Ghiorso, M. S., Lemons, R. V., & Carley, T. L. (2012). Rhyolite-MELTS: A Modified Calibration of MELTS Optimized for Silica-rich, Fluid-bearing Magmatic Systems. *Journal of Petrology*, 53(5), 875–890. <https://doi.org/10.1093/ptrology/egr080>
- Gudmundsson, A. (2007). Infrastructure and evolution of ocean-ridge discontinuities in Iceland. *Journal of Geodynamics*, 43(1), 6–29. <https://doi.org/10.1016/j.jog.2006.09.002>
- Gudmundsson, M. T., Janebo, M. H., Larsen, G., Högnadóttir, T., Thordarson, T., Gudnason, J., & Jónsdóttir, T. (2021). The explosive, basaltic Katla eruption in 1918, south Iceland II. Isopach map, ice cap deposition of tephra and layer volume. *Jökull Journal*, 71(1), 21–38. <https://doi.org/10.33799/jokull2021.71.021>
- Gudmundsson, O., Brandsdóttir, B., Menke, W., & Sigvaldason, G. E. (1994). The crustal magma chamber of the Katla volcano in south Iceland revealed by 2-D seismic undershooting. *Geophysical Journal International*, 119(1), 277–296. <https://doi.org/10.1111/j.1365-246X.1994.tb00928.x>
- Gunnarsson, B., Marsh, B. D., & Taylor, H. P. (1998). Generation of Icelandic rhyolites: Silicic lavas from the Torfajökull central volcano. *Journal of Volcanology and Geothermal Research*, 83(1–2), 1–45. [https://doi.org/10.1016/S0377-0273\(98\)00017-1](https://doi.org/10.1016/S0377-0273(98)00017-1)
- Gurenko, A. A., Bindeman, I. N., & Sigurdsson, I. A. (2015). To the origin of Icelandic rhyolites: Insights from partially melted leucocratic xenoliths. *Contributions to Mineralogy and Petrology*, 169(5), 49. <https://doi.org/10.1007/s00410-015-1145-4>
- Handley, H. K., Reagan, M., Gertisser, R., Preece, K., Berlo, K., McGee, L. E., et al. (2018). Timescales of magma ascent and degassing and the role of crustal assimilation at Merapi volcano (2006–2010), Indonesia: Constraints from uranium-series and radiogenic isotopic compositions. *Geochimica et Cosmochimica Acta*, 222, 34–52. <https://doi.org/10.1016/j.gca.2017.10.015>
- Hards, V. L., Kempton, P. D., Thompson, R. N., & Greenwood, P. B. (2000). The magmatic evolution of the Snæfell volcanic centre; an example of volcanism during incipient rifting in Iceland. *Journal of Volcanology and Geothermal Research*, 99(1–4), 97–121. [https://doi.org/10.1016/S0377-0273\(00\)00160-8](https://doi.org/10.1016/S0377-0273(00)00160-8)
- Harning, D. J., Thordarson, T., Geirsdóttir, Á., Miller, G. H., & Florian, C. R. (2024). Repeated Early Holocene eruptions of Katla, Iceland, limit the temporal resolution of the Vedde Ash. *Bulletin of Volcanology*, 86, 2. <https://doi.org/10.1007/s00445-023-01690-9>

- Hattori, K., & Muehlenbachs, K. (1982). Oxygen isotope ratios of the Icelandic crust. *Journal of Geophysical Research*, 87(B8), 6559–6565. <https://doi.org/10.1029/JB087iB08p06559>
- Heinonen, J. S., Bohron, W. A., Spera, F. J., Brown, G. A., Scruggs, M. A., & Adams, J. V. (2020). Diagnosing open-system magmatic processes using the Magma Chamber Simulator (MCS): Part II—Trace elements and isotopes. *Contributions to Mineralogy and Petrology*, 175(11), 105. <https://doi.org/10.1007/s00410-020-01718-9>
- Heinonen, J. S., Iles, K. A., Heinonen, A., Fred, R., Virtanen, V. J., Bohron, W. A., & Spera, F. J. (2021). From binary mixing to magma chamber simulator: Geochemical modeling of assimilation in magmatic systems. In M. Masotta, C. Beier, & S. Mollo (Eds.), *Crustal magmatic system evolution: Anatomy, architecture, and physico-chemical processes* (pp. 151–176). Wiley. <https://doi.org/10.1002/9781119564485.ch7>
- Hemond, C., Condomines, M., Fourcade, S., Allègre, C. J., Óskarsson, N., & Javoy, M. (1988). Thorium, strontium and oxygen isotopic geochemistry in recent tholeiites from Iceland: Crustal influence on mantle-derived magmas. *Earth and Planetary Science Letters*, 87(3), 273–285. [https://doi.org/10.1016/0012-821X\(88\)90015-5](https://doi.org/10.1016/0012-821X(88)90015-5)
- Ito, E., White, W. M., & Göpel, C. (1987). The O, Sr, Nd and Pb isotope geochemistry of MORB. *Chemical Geology*, 62(3–4), 157–176. [https://doi.org/10.1016/0009-2541\(87\)90083-0](https://doi.org/10.1016/0009-2541(87)90083-0)
- Jakobsson, S. P. (1979). Petrology of Recent Basalts of the Eastern Volcanic Zone, Iceland. In *Icelandic museum of natural history*.
- Jeddi, Z., Gudmundsson, O., & Tryggvason, A. (2017). Ambient-noise tomography of Katla volcano, south Iceland. *Journal of Volcanology and Geothermal Research*, 347, 264–277. <https://doi.org/10.1016/j.jvolgeores.2017.09.019>
- Jeddi, Z., Tryggvason, A., & Gudmundsson, Ó. (2016). The Katla volcanic system imaged using local earthquakes recorded with a temporary seismic network. *Journal of Geophysical Research: Solid Earth*, 121(10), 7230–7251. <https://doi.org/10.1002/2016JB013044>
- Jónasson, K. (2005). Magmatic evolution of the Heidarspordur ridge, NE-Iceland. *Journal of Volcanology and Geothermal Research*, 147(1–2), 109–124. <https://doi.org/10.1016/j.jvolgeores.2005.03.009>
- Jónsson, G., & Kristjánsson, L. (2000). Aeromagnetic measurements over Mýrdalsjökull and vicinity. *Jökull Journal*, 49, 47–58. <https://doi.org/10.33799/jokull2000.49.047>
- Kelley, D. F., & Barton, M. (2008). Pressures of Crystallization of Icelandic Magmas. *Journal of Petrology*, 49(3), 465–492. <https://doi.org/10.1093/petrology/egm089>
- Kokfelt, T. F., Hoernle, K., Hauff, F., Fiebig, J., Werner, R., & Garbe-Schönberg, D. (2006). Combined Trace Element and Pb–Nd–Sr–O Isotope Evidence for Recycled Oceanic Crust (Upper and Lower) in the Iceland Mantle Plume. *Journal of Petrology*, 47(9), 1705–1749. <https://doi.org/10.1093/petrology/leg1025>
- Lacasse, C., Sigurdsson, H., Carey, S. N., Jóhannesson, H., Thomas, L. E., & Rogers, N. W. (2007). Bimodal volcanism at the Katla subglacial caldera, Iceland: Insight into the geochemistry and petrogenesis of rhyolitic magmas. *Bulletin of Volcanology*, 69(4), 373–399. <https://doi.org/10.1007/s00445-006-0082-5>
- Lacasse, C., Sigurdsson, H., Jóhannesson, H., Paterne, M., & Carey, S. (1995). Source of Ash Zone 1 in the North Atlantic. *Bulletin of Volcanology*, 57, 18–32. <https://doi.org/10.1007/BF00298704>
- Larsen, G. (2000). Holocene eruptions within the Katla volcanic system, south Iceland: Characteristics and environmental impact. *Jökull Journal*, 49, 1–28. <https://doi.org/10.33799/jokull2000.49.001>
- Larsen, G., Newton, A. J., Dugmore, A. J., & Vilmundardóttir, E. G. (2001). Geochemistry, dispersal, volumes and chronology of Holocene silicic tephra layers from the Katla volcanic system, Iceland. *Journal of Quaternary Science*, 16(2), 119–132. <https://doi.org/10.1002/jqs.587>
- Macdonald, R., McGarvie, D. W., Pinkerton, H., Smith, R. L., & Palacz, A. (1990). Petrogenetic Evolution of the Torfajökull Volcanic Complex, Iceland I. Relationship Between the Magma Types. *Journal of Petrology*, 31(2), 429–459. <https://doi.org/10.1093/petrology/31.2.429>
- Macdonald, R., Sparks, R. S. J., Sigurdsson, H., Matthey, D. P., McGarvie, D. W., & Smith, R. L. (1987). The 1875 eruption of Askja volcano, Iceland: Combined fractional crystallization and selective contamination in the generation of rhyolitic magma. *Mineralogical Magazine*, 51(360), 183–202. <https://doi.org/10.1180/minmag.1987.051.360.01>
- Macpherson, C. G., Hilton, D. R., Day, J. M. D., Lowry, D., & Grönvold, K. (2005). High-³He/⁴He, depleted mantle and low- $\delta^{18}\text{O}$, recycled oceanic lithosphere in the source of central Iceland magmatism. *Earth and Planetary Science Letters*, 233(3–4), 411–427. <https://doi.org/10.1016/j.epsl.2005.02.037>
- Martin, E., & Sigmarsson, O. (2007). Crustal thermal state and origin of silicic magma in Iceland: The case of Torfajökull, Ljósufjöll and Snæfellsjökull volcanoes. *Contributions to Mineralogy and Petrology*, 153(5), 593–605. <https://doi.org/10.1007/s00410-006-0165-5>
- Martin, E., & Sigmarsson, O. (2010). Thirteen million years of silicic magma production in Iceland: Links between petrogenesis and tectonic settings. *Lithos*, 116(1–2), 129–144. <https://doi.org/10.1016/j.lithos.2010.01.005>
- Meade, F. C., Troll, V. R., Ellam, R. M., Freda, C., Font, L., Donaldson, C. H., & Klonowska, I. (2014). Bimodal magmatism produced by progressively inhibited crustal assimilation. *Nature Communications*, 5(1), 4199. <https://doi.org/10.1038/ncomms5199>
- Meara, R. H., Thordarson, T., Pearce, N. J. G., Hayward, C., & Larsen, G. (2020). A catalogue of major and trace element data for Icelandic Holocene silicic tephra layers. *Journal of Quaternary Science*, 35(1–2), 122–142. <https://doi.org/10.1002/jqs.3173>
- Meyer, P. S., Sigurdsson, H., & Schilling, J.-G. (1985). Petrological and geochemical variations along Iceland's Neovolcanic Zones. *Journal of Geophysical Research*, 90(B12), 10043–10072. <https://doi.org/10.1029/JB090iB12p10043>
- Muehlenbachs, K., Anderson, A. T., & Sigvaldason, G. E. (1974). Low- O^{18} basalts from Iceland. *Geochimica et Cosmochimica Acta*, 38(4), 577–588. [https://doi.org/10.1016/0016-7037\(74\)90042-8](https://doi.org/10.1016/0016-7037(74)90042-8)
- Muehlenbachs, K., & Clayton, R. N. (1972). Oxygen Isotope Studies of Fresh and Weathered Submarine Basalts. *Canadian Journal of Earth Sciences*, 9(2), 172–184. <https://doi.org/10.1139/e72-014>
- Óladóttir, B. A., Larsen, G., Thordarson, T., & Sigmarsson, O. (2005). The Katla volcano S-Iceland: Holocene tephra stratigraphy and eruption frequency. *Jökull Journal*, 55(1), 53–74. <https://doi.org/10.33799/jokull2005.55.053>
- Óladóttir, B. A., Sigmarsson, O., & Larsen, G. (2018). Tephra productivity and eruption flux of the subglacial Katla volcano, Iceland. *Bulletin of Volcanology*, 80(7), 58. <https://doi.org/10.1007/s00445-018-1236-y>
- Óladóttir, B. A., Sigmarsson, O., Larsen, G., & Thordarson, T. (2008). Katla volcano, Iceland: Magma composition, dynamics and eruption frequency as recorded by Holocene tephra layers. *Bulletin of Volcanology*, 70(4), 475–493. <https://doi.org/10.1007/s00445-007-0150-5>
- Olin, P. H., & Wolff, J. A. (2010). Rare earth and high field strength element partitioning between iron-rich clinopyroxenes and felsic liquids. *Contributions to Mineralogy and Petrology*, 160(5), 761–775. <https://doi.org/10.1007/s00410-010-0506-2>
- Óskarsson, N., Helgason, Ö., & Steinthórsson, S. (1994). Oxidation state of iron in mantle-derived magmas of the Icelandic rift zone. *Hyperfine Interactions*, 91(1), 733–737. <https://doi.org/10.1007/BF02064599>
- Óskarsson, N., Sigvaldason, G. E., & Steinthórsson, S. (1982). A Dynamic Model of Rift Zone Petrogenesis and the Regional Petrology of Iceland. *Journal of Petrology*, 23(1), 28–74. <https://doi.org/10.1093/petrology/23.1.28>
- Popa, R.-G., Bachmann, O., & Huber, C. (2021). Explosive or effusive style of volcanic eruption determined by magma storage conditions. *Nature Geoscience*, 14(10), 781–786. <https://doi.org/10.1038/s41561-021-00827-9>

- Pope, E. C., Bird, D. K., & Arnórsson, S. (2013). Evolution of low¹⁸O Icelandic crust. *Earth and Planetary Science Letters*, 374, 47–59. <https://doi.org/10.1016/j.epsl.2013.04.043>
- Prestvik, T., Goldberg, S., Karlsson, H., & Grönvold, K. (2001). Anomalous strontium and lead isotope signatures in the off-rift Örefajökull central volcano in south-east Iceland: Evidence for enriched endmember(s) of the Iceland mantle plume? *Earth and Planetary Science Letters*, 190(3–4), 211–220. [https://doi.org/10.1016/S0012-821X\(01\)00390-9](https://doi.org/10.1016/S0012-821X(01)00390-9)
- Pritchard, C. J., & Larson, P. B. (2012). Genesis of the post-caldera eastern Upper Basin Member rhyolites, Yellowstone, WY: From volcanic stratigraphy, geochemistry, and radiogenic isotope modeling. *Contributions to Mineralogy and Petrology*, 164(2), 205–228. <https://doi.org/10.1007/s00410-012-0733-9>
- Radu, I. B., Skogby, H., Troll, V. R., Deegan, F. M., Geiger, H., Müller, D., & Thordarson, T. (2023). Water in clinopyroxene from the 2021 Geldingadalir eruption of the Fagradalsfjall Fires, SW-Iceland. *Bulletin of Volcanology*, 85(5), 31. <https://doi.org/10.1007/s00445-023-01641-4>
- Rasmussen, M. B., Halldórsson, S. A., Jackson, M. G., Bindeman, I. N., & Whitehouse, M. J. (2022). Helium and oxygen isotopic variations in the Iceland plume source controlled by entrainment of recycled oceanic lithosphere. *Earth and Planetary Science Letters*, 594, 117691. <https://doi.org/10.1016/j.epsl.2022.117691>
- Riisshuus, M. S., Harris, C., Peate, D. W., Tegner, C., Wilson, J. R., & Brooks, C. K. (2015). Formation of low- $\delta^{18}\text{O}$ magmas of the Kangerlussuaq Intrusion by addition of water derived from dehydration of foundered basaltic roof rocks. *Contributions to Mineralogy and Petrology*, 169(5), 41. <https://doi.org/10.1007/s00410-015-1134-7>
- Rollinson, H. R. (1993). *Using geochemical data: Evaluation, presentation, interpretation*. Longman Scientific and Technical.
- Schattel, N., Portnyagin, M., Golowin, R., Hoernle, K., & Bindeman, I. (2014). Contrasting conditions of rift and off-rift silicic magma origin on Iceland. *Geophysical Research Letters*, 41(16), 5813–5820. <https://doi.org/10.1002/2014GL060780>
- Seligman, A. N., Bindeman, I. N., McClaughry, J., Stern, R. A., & Fisher, C. (2014). The earliest low and high $\delta^{18}\text{O}$ caldera-forming eruptions of the Yellowstone plume: Implications for the 30–40 Ma Oregon calderas and speculations on plume-triggered delaminations. *Frontiers in Earth Science*, 2, 34. <https://doi.org/10.3389/feart.2014.00034>
- Sigmarrsson, O., Condomines, M., & Fourcade, S. (1992). A detailed Th, Sr and O isotope study of Hekla: Differentiation processes in an Icelandic Volcano. *Contributions to Mineralogy and Petrology*, 112(1), 20–34. <https://doi.org/10.1007/BF00310953>
- Sigmarrsson, O., Hémond, C., Condomines, M., Fourcade, S., & Óskarsson, N. (1991). Origin of silicic magma in Iceland revealed by Th isotopes. *Geology*, 19(6), 621–624. [https://doi.org/10.1130/0091-7613\(1991\)019%3C0621:OOSMII%3E2.3.CO;2](https://doi.org/10.1130/0091-7613(1991)019%3C0621:OOSMII%3E2.3.CO;2)
- Sigmarrsson, O., Vlastelic, I., Andreassen, R., Bindeman, I., Devidal, J.-L., Moune, S., et al. (2011). Remobilization of silicic intrusion by mafic magmas during the 2010 Eyjafjallajökull eruption. *Solid Earth*, 2(2), 271–281. <https://doi.org/10.5194/se-2-271-2011>
- Sigmundsson, F., Hreinsdóttir, S., Hooper, A., Árnadóttir, T., Pedersen, R., Roberts, M. J., et al. (2010). Intrusion triggering of the 2010 Eyjafjallajökull explosive eruption. *Nature*, 468, 426–430. <https://doi.org/10.1038/nature09558>
- Sigurdsson, H. (1968). Petrology of acid xenoliths from Surtsey. *Geological Magazine*, 105(5), 440–453. <https://doi.org/10.1017/S0016756800054820>
- Sigurdsson, H. (1977). Generation of Icelandic rhyolites by melting of plagiogranites in the oceanic layer. *Nature*, 269(5623), 25–28. <https://doi.org/10.1038/269025a0>
- Sigurdsson, H., & Sparks, R. S. J. (1981). Petrology of Rhyolitic and Mixed Magma Ejecta from the 1875 Eruption of Askja, Iceland. *Journal of Petrology*, 22(1), 41–84. <https://doi.org/10.1093/ptrology/22.1.41>
- Soosalu, H., Jónsdóttir, K., & Einarsson, P. (2006). Seismicity crisis at the Katla volcano, Iceland—Signs of a cryptodome? *Journal of Volcanology and Geothermal Research*, 153(3–4), 177–186. <https://doi.org/10.1016/j.jvolgeores.2005.10.013>
- Stecher, O., Carlson, R. W., & Gunnarsson, B. (1999). Torfajökull: A radiogenic end-member of the Iceland Pb-isotopic array. *Earth and Planetary Science Letters*, 165(1), 117–127. [https://doi.org/10.1016/S0012-821X\(98\)00256-8](https://doi.org/10.1016/S0012-821X(98)00256-8)
- Stimac, J., & Hickmott, D. (1994). Trace-element partition coefficients for ilmenite, orthopyroxene and pyrrhotite in rhyolite determined by micro-PIXE analysis. *Chemical Geology*, 117(1–4), 313–330. [https://doi.org/10.1016/0009-2541\(94\)90134-1](https://doi.org/10.1016/0009-2541(94)90134-1)
- Sturkell, E., Einarsson, P., Roberts, M. J., Geirsson, H., Gudmundsson, M. T., Sigmundsson, F., et al. (2008). Seismic and geodetic insights into magma accumulation at Katla subglacial volcano, Iceland: 1999 to 2005. *Journal of Geophysical Research*, 113(B3), B03212. <https://doi.org/10.1029/2006JB004851>
- Sturkell, E., Einarsson, P., Sigmundsson, F., Hooper, A., Ófeigsson, B. G., Geirsson, H., & Ólafsson, H. (2010). Katla and Eyjafjallajökull volcanoes. In *Developments in Quaternary Sciences* (Vol. 13, pp. 5–21). Elsevier. [https://doi.org/10.1016/S1571-0866\(09\)01302-5](https://doi.org/10.1016/S1571-0866(09)01302-5)
- Sun, S.-S., & McDonough, W. F. (1989). Chemical and isotopic systematics of oceanic basalts: Implications for mantle composition and processes. *Geological Society, London, Special Publications*, 42(1), 313–345. <https://doi.org/10.1144/GSL.SP.1989.042.01.19>
- Svanholm, C. (2021). *Origin of silicic magmatism at the Katla Volcano, South Iceland* (Bachelor's thesis). Uppsala University.
- Takach, M. K., Bohron, W. A., Spera, F. J., & Viccaro, M. (2024). The Role of Crustal Contamination throughout the 1329–2005 CE Eruptive Record of Mt. Etna Volcano, Italy. *Journal of Petrology*, 65(4), egae028. <https://doi.org/10.1093/ptrology/egae028>
- Taylor, H. P., Jr., & Sheppard, S. M. F. (1986). Igneous rocks: I. Processes of isotopic fractionation and isotope systematics. In J. W. Valley, H. P. Taylor, & J. R. O'Neil (Eds.), *Stable isotopes in high temperature geological processes* (pp. 227–272). De Gruyter. <https://doi.org/10.1515/9781501508936-013>
- Thirlwall, M. F., Gee, M. A. M., Lowry, D., Matthey, D. P., Murton, B. J., & Taylor, R. N. (2006). Low $\delta^{18}\text{O}$ in the Icelandic mantle and its origins: Evidence from Reykjanes Ridge and Icelandic lavas. *Geochimica et Cosmochimica Acta*, 70(4), 993–1019. <https://doi.org/10.1016/j.gca.2005.09.008>
- Thordarson, T., & Höskuldsson, Á. (2008). Postglacial volcanism in Iceland. *Jökull Journal*, 58, 197–228. <https://doi.org/10.33799/jokull2008.58.197>
- Thordarson, T., Miller, D. J., Larsen, G., Self, S., & Sigurdsson, H. (2001). New estimates of sulfur degassing and atmospheric mass-loading by the 934 AD Eldgjá eruption, Iceland. *Journal of Volcanology and Geothermal Research*, 108(1–4), 33–54. [https://doi.org/10.1016/S0377-0273\(00\)00277-8](https://doi.org/10.1016/S0377-0273(00)00277-8)
- Tomlinson, E. L., Thordarson, T., Lane, C. S., Smith, V. C., Manning, C. J., Müller, W., & Menzies, M. A. (2012). Petrogenesis of the Sólheimar ignimbrite (Katla, Iceland): Implications for tephrostratigraphy. *Geochimica et Cosmochimica Acta*, 86, 318–337. <https://doi.org/10.1016/j.gca.2012.03.012>
- Torsvik, T. H., Amundsen, H. E. F., Trønnes, R. G., Doubrovine, P., Gaina, C., Kuszniir, N. J., et al. (2015). Continental crust beneath southeast Iceland. *Proceedings of the National Academy of Sciences of the United States of America*, 112(15), E1818–E1827. <https://doi.org/10.1073/pnas.1423099112>

- Troch, J., Ellis, B. S., Harris, C., Ulmer, P., Bouvier, A.-S., & Bachmann, O. (2019). Experimental Melting of Hydrothermally Altered Rocks: Constraints for the Generation of Low- $\delta^{18}\text{O}$ Rhyolites in the Central Snake River Plain. *Journal of Petrology*, *60*(10), 1881–1902. <https://doi.org/10.1093/petrology/egz056>
- Troll, V. R., Chadwick, J. P., Ellam, R. M., Mc Donnell, S., Emeleus, C. H., & Meighan, I. G. (2005). Sr and Nd isotope evidence for successive crustal contamination of Slieve Gullion ring-dyke magmas, Co. Armagh, Ireland. *Geological Magazine*, *142*(6), 659–668. <https://doi.org/10.1017/S0016756805001068>
- Troll, V. R., Deegan, F. M., Heinonen, J. S., Svanholm, C., Harris, C., Lacasse, C. M., et al. (2025). Origin of Silicic Magmatism at the Katla Volcanic Complex, South Iceland (Version 1) [Dataset]. *Zenodo*. <https://doi.org/10.5281/zenodo.15039180>
- Troll, V. R., Deegan, F. M., Thordarson, T., Tryggvason, A., Krmíček, L., Moreland, W. M., et al. (2024). The Fagradalsfjall and Sundhnúkur Fires of 2021–2024: A single magma reservoir under the Reykjanes Peninsula, Iceland? *Terra Nova*, *36*(6), 447–456. <https://doi.org/10.1111/ter.12733>
- Troll, V. R., Donaldson, C. H., & Emeleus, C. H. (2004). Pre-eruptive magma mixing in ash-flow deposits of the Tertiary Rum Igneous Centre, Scotland. *Contributions to Mineralogy and Petrology*, *147*(6), 722–739. <https://doi.org/10.1007/s00410-004-0584-0>
- Troll, V. R., Nicoll, G. R., Ellam, R. M., Emeleus, C. H., & Mattsson, T. (2021). Petrogenesis of the Loch Bà ring-dyke and Centre 3 granites, Isle of Mull, Scotland. *Contributions to Mineralogy and Petrology*, *176*(2), 16. <https://doi.org/10.1007/s00410-020-01763-4>
- Valley, J. W., Lackey, J. S., Cavosie, A. J., Clechenko, C. C., Spicuzza, M. J., Basei, M. A. S., et al. (2005). 4.4 billion years of crustal maturation: Oxygen isotope ratios of magmatic zircon. *Contributions to Mineralogy and Petrology*, *150*(6), 561–580. <https://doi.org/10.1007/s00410-005-0025-8>
- Vennemann, T. W., & Smith, H. S. (1990). The rate and temperature of reaction of ClF_3 with silicate minerals, and their relevance to oxygen isotope analysis. *Chemical Geology: Isotope Geoscience section*, *86*(1), 83–88. [https://doi.org/10.1016/0168-9622\(90\)90008-Z](https://doi.org/10.1016/0168-9622(90)90008-Z)
- Walker, G. P. L. (1966). Acid volcanic rocks in Iceland. *Bulletin Volcanologique*, *29*(1), 375–402. <https://doi.org/10.1007/BF02597164>
- Watts, K. E., Bindeman, I. N., & Schmitt, A. K. (2012). Crystal scale anatomy of a dying supervolcano: An isotope and geochronology study of individual phenocrysts from voluminous rhyolites of the Yellowstone caldera. *Contributions to Mineralogy and Petrology*, *164*(1), 45–67. <https://doi.org/10.1007/s00410-012-0724-x>
- Winpenny, B., & MacLennan, J. (2014). Short Length Scale Oxygen Isotope Heterogeneity in the Icelandic Mantle: Evidence from Plagioclase Compositional Zones. *Journal of Petrology*, *55*(12), 2537–2566. <https://doi.org/10.1093/petrology/egu066>
- Zierenberg, R. A., Schiffman, P., Barfod, G. H., Leshner, C. E., Marks, N. E., Lowenstern, J. B., et al. (2013). Composition and origin of rhyolite melt intersected by drilling in the Krafla geothermal field, Iceland. *Contributions to Mineralogy and Petrology*, *165*(2), 327–347. <https://doi.org/10.1007/s00410-012-0811-z>